Forschungszentrum Jülich

Institut für Plasmaphysik
EURATOM Association, Trilateral Euregio Cluster

The CRMOL Manual: Collisional-radiative models for molecular hydrogen in plasmas

Philip Thornton Greenland

Jül-3858

The CRMOL Manual: Collisional-radiative models for molecular hydrogen in plasmas

Philip Thornton Greenland

Berichte des Forschungszentrums Jülich ; 3858
ISSN 0944-2952
Institut für Plasmaphysik Jül-3858
EURATOM Association, Mitglied im Trilateral Euregio Cluster

Zu beziehen durch: Forschungszentrum Jülich GmbH · Zentralbibliothek
52425 Jülich · Bundesrepublik Deutschland
☎ 02461/61-5220 · Telefax: 02461/61-6103 · e-mail: zb-publikation@fz-juelich.de

The CRMOL Manual: Collisional-radiative models for molecular hydrogen in plasmas

P T Greenland
Optics Section, Blackett Laboratory,
Imperial College, London SW7 2BZ, UK, and
Department of Physics and Astronomy,
University College London WC1E 6BT, UK

Abstract

This manual describes the code `crmol` a collisional-radiative modelling code which produces effective rate coefficients and population coefficients for the analysis of hydrogen, including molecular hydrogen, in plasmas. The manual comprises six sections

1. Introduction
2. A mathematical definition of what `crmol` is supposed to do, and some proofs relevant to the validity of collisional-radiative models. Most of the rest of the manual can be used without a detailed understanding of this section.
3. Instructions for running the code, the most relevant part for users.
4. Details of electron energy loss rates, which are also calculated by the code.
5. Discussions on validity and accuracy.
6. A detailed example, showing how the code can be used to calculate the number of Fulcher band photons/molecular loss.

and three appendicies giving details of the data used in the code.

Contents

1 Introduction

This is the `crmol` manual, which describes the current version `crmol`, including the theoretical basis of the code, the sources of its atomic and molecular data and its use.

Collisional radiative models (CR models) have been used in plasma physics for a long time. Originally the term was used in astrophysical applications to describe an approximation which quantified the equilibrium state for plasma densities higher than those for 'coronal equilibrium' but not yet high enough for 'Saha equilibrium', and the same approximations were later used for plasma states characterized by a 'transport equilibrium' (rather than an equilibrium determined by atomic processes). The CR model is supposed to provide effective ionisation rates, recombination rates *etc* — the'collision radiative rates' — which implicitly account for collisional processes which are fast enough not to require explicit treatment in transport equations (Reiter 1993). The terms 'multistep ionisation/recombination', or 'ladderlike ionisation/recombination'are also sometimes used.

As long as only hydrogen atoms are considered under low opacity conditions the procedure to set up these rates is well known (Johnson, 1972). Sawada and Fujimoto (1995) have developed a CR model which includes the effects of transitions between electronically excited molecular states, and their model was further extended by Greenland and Reiter (1996), to include transitions between vibrational levels of the electronic ground state of the molecule. Effective rates derived from this model were given by Reiter *et al.* (1997), and were used to discuss 'molecular activated recombination' (MAR), a process suggested by Krasheninnikov *et al* (1996, 1997).

However, the full complexity of a CR model which includes molecular hydrogen has only recently been exposed. The mathematical details are discussed in some detail by Greenland (2000), and are only repeated here in order to enable the use of the program `crmol` to be described and understood. An important feature of `crmol` is its internal assesment of the validity of the effective rate coefficients and population coefficients which it generates.

Section 2 is a mathematical description of details of the CR model. It gives derives the circumstances under which a CR model is valid, and therefore specifies a precice definition of the accuracy criteria *etc.* However it is not necessary to follow the derivations given there in detail in order to use the code. Section 3 describes the use of the code, and describes the input and output required to obtain effective CR rate coefficients as well as the population coefficients. In section 4 the energy loss rates implied by the CR rate coefficients are discussed, and in section 5 the validity and accuracy of the CR model are treated. Section 6 shows some details of a practical calculation, and the data used in the code is assembled in appendicies at the end.

2 Mathematics of CR models

We start with a set of non-linear rate equations for the densities of the plasma components. These have the form

$$\dot{n}_k = \sum_{i,j} \mathcal{R}^k_{i,j}(T) n_i n_j + \sum_j A^k_j n_j - n_k \sum_{i,j} \mathcal{R}^j_{i,k}(T) n_i - n_k \sum_j A^j_k + \Gamma_k \quad (1)$$

where n_k is the density of species k, $\mathcal{R}^k_{i,j}(T)$ is the rate coefficient for production of species k from collisions between species i and j at plasma temperature T, A^k_j is the Einstein A coefficient for radiative decay from $j \rightarrow k$ and Γ_k is an external source of species k. In all that follows I shall assume that $\dot{n}_k = dn_k/dt$ and that $n_k(t)$ is a function of time only so that equation (1) represents a set of non-linear ordinary differential equations. The more general case, $\dot{n}_k = \partial n_k/\partial t + \mathbf{v}_k \cdot \nabla$, with $n_k(\mathbf{x}, t)$ a function of both space and time, so that 1 is a set of non-linear partial differential equations will not be considered. However it is clear that much of the discussion below also applies to this case.

In order to make a collisional-radiative (CR) model, these equations must first be linearized. This is done by *fixing* selected densities. We assume we can divide the species into two classes $\{I\}$ and $\{J\}$ such that only collisions of the types

$$i_1 + j_1 \rightarrow j_2 \quad (2)$$

$$i_1 + j_1 \rightarrow i_2 \quad (3)$$

$$i_1 + i_2 \rightarrow i_3 \quad (4)$$

but *not*

$$j_1 + j_2 \rightarrow j_3 \quad (5)$$

occur, where, of course

$$i_1, i_2, i_3 \cdots \in \{I\} \quad (6)$$

and

$$j_1, j_2, j_3 \cdots \in \{J\} \quad (7)$$

Then if we *fix* the densities of all species $i \in \{I\}$, equation 1 will reduce to a set of*linear* rate equations for the species $j \in \{J\}$. Notice that this requires that we can choose $\{I\}$ and $\{J\}$ so that all rate coefficients of the form

$$\mathcal{R}^{j_3}_{j_1,j_2} = 0 \quad (8)$$

Equation 1 now becomes

$$\dot{n}_{j_3} = A + B + \Gamma_{\mathrm{CR}} + \Gamma_{j_3} \quad (9)$$

with

$$A = \sum_{i_1,j_2} \mathcal{R}^{j_3}_{i_1,j_2} N_{i_1} n_{j_2} + \sum_{j_2} A^{j_3}_{j_2} n_{j_2} - n_{j_3} \sum_{i,j_2} \mathcal{R}^{j_2}_{i,j_3} N_i - n_{j_3} \sum_{j_2} A^{j_2}_{j_3} \quad (10)$$

$$B = -n_{j_3} \sum_{i_1,i_2} \mathcal{R}^{i_2}_{i_1,j_3} N_{i_2} - n_{j_3} \sum_{i_2} A^{i_2}_{j_3} \tag{11}$$

and

$$\Gamma_{\rm CR} = \sum_{i_1,i_2} \mathcal{R}^{j_3}_{i_1,i_2} N_{i_1} N_{i_2} + \sum_{i_2} A^{j_3}_{i_2} N_{i_2} \tag{12}$$

Here we have written the fixed densities $\in \{I\}$) in upper case. It is easy to see that the term A (eq. 5b) represents population changes due to collisions between species $\{I\}$ and $\{J\}$, and decay within species $\{J\}$, B (eq. 5c) represents loss of species $\{J\}$ due to collisional conversion or decay to species $\{I\}$, and $\Gamma_{\rm CR}$ (equation 12) is an extra source term which derives from collisions and decays amongst species $\{I\}$ leading to species $\{J\}$.

A common situation is that in which the electron density is fixed, and the rate equations for *eg* H atoms and protons are considered. In this case $\{I\}$ contains only 1 member and equation 8 is satisfied as long as atom-atom and atom-proton collisions are ignored. The source term $\Gamma_{\rm CR}$ is zero, the term A contains electron impact excitation, de-excitation, ionization and recombination. The term B is empty.

However, if both electron-atom and proton-atom collisions are to be included, then both the electron and proton densities must be fixed, equation 8 is satisfied as long as atom-atom collisions are ignored, the term A includes both electron-atom and proton-atom collisional excitation and de-excitation, but not recombination or ionization. The term B contains the loss of atoms due to both electron and proton impact ionization, and $\Gamma_{\rm CR}$ contains electron-proton recombination. Charge exchange appears in A. From the point of view of atomic populations it is a special kind of atomic excitation.

The purpose of this exercise is to extract a set of l *linear* rate equations from 1. They may now be written in matrix form as

$$\dot{\mathbf{n}} = \mathbf{M}(N_1 \cdots N_K)\mathbf{n} + \mathbf{\Gamma}_{\rm CR}(N_1 \cdots N_K) + \mathbf{\Gamma} \tag{13}$$

with initial conditions specified by $\mathbf{n}(0)$.

Here we have indicated that the $l \times l$ rate matrix $\mathbf{M}(N_1 \cdots N_K)$ and the l vector $\mathbf{\Gamma}_{\rm CR}(N_1 \cdots N_K)$ both depend upon the K fixed densities $N_1 \cdots N_K$.

Now the full dynamics of the system can be solved if the l equations 13 are supplemented with the K equations for the 'fixed' densities $N_1 \cdots N_K$ (which can be derived from 1), but this of course does not lead to any simplification. The task is to use the linearity of the equation 13 to construct a CR model based on its l components. If this is done correctly it will produce $l'(\ll l)$ coupled linear equations with effective rate coefficients which are (very non-linear) functions of the fixed densities $N_1 \cdots N_K$. The dynamics of the system can then be described by the $l' + K$ equations for the reduced system, and the hope is that they will be easier to solve than the original much larger set of $l + K$ equations.

The details of how a CR model can be derived from equation 13 are described in Greenland (2000). Briefly, we divide the l states represented in equation 13 into two classes, a P class and a Q class, so that, notionally, the P class contains the slowly varying populations whereas the Q class contains the rapidly varying populations. We define two projection operators P and Q, which project out the classes. For convenience we order the states, and therefore M so that the P states come first, and the Q states second, so that 13 becomes

$$\begin{bmatrix} \dot{\mathbf{n}}_P \\ \dot{\mathbf{n}}_Q \end{bmatrix} = \begin{bmatrix} \mathrm{M}_P & \mathbf{H} \\ \mathbf{V} & \mathrm{M}_Q \end{bmatrix} \begin{bmatrix} \mathbf{n}_P \\ \mathbf{n}_Q \end{bmatrix} + \mathbf{\Gamma}_{\mathbf{CR}} + \mathbf{\Gamma} \tag{14}$$

where $P\mathrm{M}P = \mathrm{M}_P$, $P\mathrm{M}Q = \mathbf{H}$, $Q\mathrm{M}P = \mathbf{V}$, $Q\mathrm{M}Q = \mathrm{M}_Q$, $\mathbf{n}_P = P\mathbf{n}$ and $\mathbf{n}_Q = Q\mathbf{n}$. The rows in the vectors $\mathbf{\Gamma}_{\mathbf{CR}}$ and $\mathbf{\Gamma}$ are permuted accordingly. We assume that there are N_P P states and N_Q Q states, so that $N_P + N_Q = l$.

All the criteria for a valid CR model can be derived by considering the equation

$$\dot{\mathbf{n}} = \mathrm{M}\mathbf{n} + \mathbf{\Gamma} \tag{15}$$

whose solution is

$$\mathbf{n}(t) = \exp(\mathrm{M}t)\mathbf{n}(0) + \exp(\mathrm{M}t) \int_0^t \exp(-\mathrm{M}t')\, dt'\ \mathbf{\Gamma} \tag{16}$$

This is supposed to be adequatly approximated by

$$\mathbf{n}_P(t) = \exp(\mathrm{M}_{\mathrm{eff}}t)\mathbf{n}'_P(0) + \exp(\mathrm{M}_{\mathrm{eff}}t) \int_0^t \exp(-\mathrm{M}_{\mathrm{eff}}t')\, dt'\ \mathbf{\Gamma}'_P \tag{17}$$

$$\mathbf{n}_Q(t) = \mathcal{O}\mathbf{n}_P(t) - \mathrm{M}_Q^{-1}\mathbf{\Gamma}_Q \tag{18}$$

so that $\mathbf{n}_P$ satisfies

$$\dot{\mathbf{n}}_P = \mathrm{M}_{\mathrm{eff}}\mathbf{n}_P + \mathbf{\Gamma}'_P \tag{19}$$

with initial condition $\mathbf{n}'(0)$, where the quantities $\mathbf{n}'_P(0)$ $\mathbf{\Gamma}'_P$ and $\mathcal{O}$ are defined below. We shall see that, provided a correction for the Q space component of Γ is made, this is indeed true.

A proper discussion of these solutions requires knowledge of the eigen*vectors* of M as well as the eigenvalues. We define $\mathbf{T}$ as an $N \times N$ matrix whose columns are the normalized eigenvectors of M, arranged in order of increasing absolute value of the eigenvalues and

$$\mathbf{D} = \mathrm{diag}\left\{\lambda^{(1)}, \lambda^{(2)}, \cdots \lambda^{(N)}\right\} \tag{20}$$

as the diagonal matrix of eigenvalues $\lambda^{(k)}$, also in increasing order of absolute magnitude.

It is convenient to subdivide $\mathbf{T}$ as

$$\mathbf{T} = \begin{bmatrix} \mathbf{T}_P & \mathbf{\Delta} \\ \delta & \mathbf{T}_Q \end{bmatrix} \tag{21}$$

where $\mathbf{T}_P$ is an $N_P \times N_P$ submatrix, so that, $\mathbf{T}_P$ represents the P space part of the eigenvectors which correspond to the P space eigenvalues. Similarly $\mathbf{T}_Q$ is the $N_Q \times N_Q$ submatrix which represents the Q space part of the eigenvectors which correspond to the Q space eigenvalues. $\mathbf{\Delta}$ is the P space part of the eigenvectors corresponding to the Q space eigenvalues and δ the Q space part of the eigenvectors corresponding to the P space eigenvalues.

Similarly, defining

$$\mathbf{D}_P = \text{diag}\left\{\lambda^{(1)}, \lambda^{(2)}, \cdots \lambda^{(N_P)}\right\} \tag{22}$$

and

$$\mathbf{D}_Q = \text{diag}\left\{\lambda^{(N_P+1)}, \lambda^{(N_P+2)}, \cdots \lambda^{(N)}\right\} \tag{23}$$

we get

$$\mathbf{MT} = \begin{bmatrix} \mathbf{M}_P & \mathbf{H} \\ \mathbf{V} & \mathbf{M}_Q \end{bmatrix} \begin{bmatrix} \mathbf{T}_P & \mathbf{\Delta} \\ \delta & \mathbf{T}_Q \end{bmatrix} = \begin{bmatrix} \mathbf{T}_P & \mathbf{\Delta} \\ \delta & \mathbf{T}_Q \end{bmatrix} \begin{bmatrix} \mathbf{D}_P & \mathbf{0} \\ \mathbf{0} & \mathbf{D}_Q \end{bmatrix} = \mathbf{TD} \tag{24}$$

By performing the block matrix multiplications, and defining

$$\mathbf{M}_{\text{eff}} = [\mathbf{M}_P - \mathbf{H}\mathbf{M}_Q^{-1}\mathbf{V}] \tag{25}$$

it is straightforward to show that

$$\mathbf{M}_{\text{eff}}\mathbf{T}_P = \left[\mathbf{1} - \mathbf{H}\mathbf{M}_Q^{-1}\delta\mathbf{T}_P^{-1}\right]\mathbf{T}_P\mathbf{D}_P \tag{26}$$

Now, in general, $\mathbf{H}\mathbf{M}_Q^{-1} \sim 1$, and since $\mathbf{T}$ is constructed from normalized eigenvectors, if[1]

$$\delta \ll 1 \tag{27}$$

then $\mathbf{T}_P \sim 1$ so that $\mathbf{T}_P^{-1} \sim 1$ and so, to a good approximation

$$\mathbf{M}_{\text{eff}}\mathbf{T}_P = [\mathbf{T}_P + O(\delta)]\mathbf{D}_P \tag{28}$$

Thus, only if $\delta \ll 1$, then the P space part of the eigenvectors corresponding to the P space eigenvalues are, to an adequate approximation the eigenvectors

[1] I define the size of column n of length m in an $m \times n$ matrix $v_{m,n}$ through the l_1 (Manhatten) norm $||\mathbf{v}||_1^{(n)}$ *viz*

$$||\mathbf{v}||_1^{(n)} = \sum_{k=1}^{m} |v_{k,n}|$$

and the 'size' of the matrix $\mathbf{v}$ as $\max_n\{||\mathbf{v}||_1^{(n)}\}$. This definition is used in expressions involving $\ll \delta$ *etc.*

of $\mathrm{M}_{\mathrm{eff}}$, with eigenvalues $\lambda^{(k)}$, $k = 1 \cdots N_P$. This, as we shall see, is a key requirement[2]. Furthermore, if both $\delta \ll 1$ *and* $\mathbf{T}_Q^{-1}\delta \ll 1$, we can write

$$\mathbf{T}^{-1} = \begin{bmatrix} \mathbf{T}_P^{-1} & -\mathbf{T}_P^{-1}\boldsymbol{\Delta}\mathbf{T}_Q^{-1} \\ -\mathbf{T}_Q^{-1}\delta\mathbf{T}_P^{-1} & \mathbf{T}_Q^{-1} \end{bmatrix} \tag{29}$$

which enables us to write (for $\delta \ll 1$, $\mathbf{T}_Q^{-1}\delta \ll 1$)

$$\mathrm{M} = \begin{bmatrix} \mathbf{T}_P\left\{\mathbf{D}_P - \mathbf{T}_P^{-1}\boldsymbol{\Delta}\mathbf{D}_Q\mathbf{T}_Q^{-1}\delta\right\}\mathbf{T}_P^{-1} & -\mathbf{T}_P\left\{\mathbf{D}_P\mathbf{T}_P^{-1}\delta - \mathbf{T}_P^{-1}\boldsymbol{\Delta}\mathbf{D}_Q\right\}\mathbf{T}_Q^{-1} \\ -\mathbf{T}_Q\left\{\mathbf{D}_Q\mathbf{T}_Q^{-1}\delta - \mathbf{T}_Q^{-1}\delta\mathbf{D}_P\right\}\mathbf{T}_P^{-1} & \mathbf{T}_Q\left\{\mathbf{D}_Q - \mathbf{T}_Q^{-1}\delta\mathbf{D}_P\mathbf{T}_P^{-1}\boldsymbol{\Delta}\right\}\mathbf{T}_Q^{-1} \end{bmatrix} \tag{30}$$

Now $\exp(\mathrm{M}t)$ for $t \gg 1/|\lambda^{(N_P+1)}|$ can be obtained from 21 by making the replacements

$$\mathbf{D}_P \rightarrow \mathbf{E}t = \mathrm{diag}\left\{\exp(\lambda^{(1)}t), \exp(\lambda^{(2)}t), \cdots \exp(\lambda^{(N_P)}t)\right\} \tag{31}$$

and

$$\mathbf{D}_Q \rightarrow \mathbf{0} \tag{32}$$

to give

$$\exp(\mathrm{M}t) = \begin{bmatrix} \mathbf{T}_P\mathbf{E}t\mathbf{T}_P^{-1} & -\mathbf{T}_P\mathbf{E}t\mathbf{T}_P^{-1}\delta\mathbf{T}_Q^{-1} \\ \delta\mathbf{E}t\mathbf{T}_P^{-1} & -\delta\mathbf{E}t\mathbf{T}_P^{-1}\boldsymbol{\Delta}\mathbf{T}_Q^{-1} \end{bmatrix} \tag{33}$$

or

$$\{\exp(\mathrm{M}t)\mathbf{n}(0)\}_P = \mathbf{n}_P(t) = \exp(\mathrm{M}_{\mathrm{eff}}t)\mathbf{n}'_P(0) \tag{34}$$

with

$$\mathbf{n}'_P(0) = \mathbf{n}_P(0) - \boldsymbol{\Delta}\mathbf{T}_Q^{-1}\mathbf{n}_Q(0) \tag{35}$$

and

$$\{\exp(\mathrm{M}t)\mathbf{n}(0)\}_Q = \delta\mathbf{T}_P^{-1}\mathbf{n}_P(t) \tag{36}$$

as well as

$$\left\{\exp(\mathrm{M}t)\int_0^t \exp(-\mathrm{M}t')\,dt'\;\boldsymbol{\Gamma}\right\}_P = \exp(\mathrm{M}_{\mathrm{eff}}t)\int_0^t \exp(-\mathrm{M}_{\mathrm{eff}}t')\,dt'\;\boldsymbol{\Gamma}'_P + C_P \tag{37}$$

with

$$\boldsymbol{\Gamma}'_P = \boldsymbol{\Gamma}_P - \boldsymbol{\Delta}\mathbf{T}_Q^{-1}\boldsymbol{\Gamma}_Q \tag{38}$$

and

$$\left\{\exp(\mathrm{M}t)\int_0^t \exp(-\mathrm{M}t')\,dt'\;\boldsymbol{\Gamma}\right\}_Q =$$

$$\delta\mathbf{T}_P^{-1}\exp(\mathrm{M}_{\mathrm{eff}}t)\int_0^t \exp(-\mathrm{M}_{\mathrm{eff}}t')\,dt'\;\boldsymbol{\Gamma}'_P - \mathrm{M}_Q^{-1}\{1 + O(\delta)\}\boldsymbol{\Gamma}_Q \tag{39}$$

[2]We can also show that

$$\mathbf{M}_Q\mathbf{T}_Q\left[\mathbf{1} - \mathbf{T}_Q^{-1}\delta\mathbf{T}_P^{-1}\boldsymbol{\Delta}\right] = \mathbf{T}_Q\mathbf{D}_Q\left[\mathbf{1} - \mathbf{D}_Q^{-1}\mathbf{T}_Q^{-1}\delta\mathbf{D}_P\mathbf{T}_P^{-1}\boldsymbol{\Delta}\right]$$

so that if $\mathbf{T}_Q^{-1}\delta \ll 1$, $\mathbf{T}_Q$ represents the eigenvectors of $\mathbf{M}_Q$

so that

$$\mathcal{O} = \delta \mathbf{T}_P^{-1} \tag{40}$$

We also have

$$\mathcal{C}_P = -\boldsymbol{\Delta} \mathbf{T}_Q^{-1} \mathbf{M}_Q^{-1} \boldsymbol{\Gamma}_Q \tag{41}$$

as the correction mentioned above. Physically, it corresponds to the contribution which arises from the equilibration of the Q space part of the source term on a timescale less than τ_Q.

The 'traditional' CR model reproduces equation 19, but with initial conditions specified by

$$\mathbf{n}_P(0) - \mathbf{H} \mathbf{M}_Q^{-1} \mathbf{n}_Q(0) \tag{42}$$

and the excited state densities determined by

$$\mathbf{n}_Q(t) = -\mathbf{M}_Q^{-1} \mathbf{V} \mathbf{n}_P(t) - \mathbf{M}_Q^{-1} \boldsymbol{\Gamma}_Q \tag{43}$$

Thus, only if we can show that

$$\delta \mathbf{T}_P^{-1} = -\mathbf{M}_Q^{-1} \mathbf{V} \tag{44}$$

$$\boldsymbol{\Delta} \mathbf{T}_Q^{-1} = \mathbf{H} \mathbf{M}_Q^{-1} \tag{45}$$

and $\mathcal{C}_P$ and is negligible will the solution of (15) be adequately given by the solution of (19) using (42) to (43) so that the traditional CR model will be valid. Equation (24) implies

$$\mathbf{V} \mathbf{T}_P + \mathbf{M}_Q \delta = \delta \mathbf{D}_P \tag{46}$$

which is easily manipulated to give

$$\delta \mathbf{T}_P^{-1} = -\mathbf{M}_Q^{-1} \mathbf{V} + \mathbf{M}_Q^{-1} \delta \mathbf{T}_P^{-1} \mathbf{M}_{\text{eff}} \tag{47}$$

Similarly by considering the left eigenvector analogue of equation (24)

$$\mathbf{T}^{-1} \mathbf{M} = \mathbf{D} \mathbf{T}^{-1}$$

and expression 20, we see

$$\mathbf{T}_P^{-1} \mathbf{H} - \mathbf{T}_P^{-1} \boldsymbol{\Delta} \mathbf{T}_Q^{-1} \mathbf{M}_Q = -\mathbf{D}_P \mathbf{T}_P^{-1} \boldsymbol{\Delta} \mathbf{T}_Q^{-1} \tag{48}$$

whence we get

$$\boldsymbol{\Delta} \mathbf{T}_Q^{-1} = \mathbf{H} \mathbf{M}_Q^{-1} + \mathbf{M}_{\text{eff}} \boldsymbol{\Delta} \mathbf{T}_Q^{-1} \mathbf{M}_Q^{-1} \tag{49}$$

Neither equations (44) nor (45) can be derived from the smallness of δ. However, as equations (47) and (49) show, these equations are satisfied (and $\mathcal{C}_P$ is negligible) if

$$|\lambda^{(N_P)}| \ll |\lambda^{(N_P+1)}| \tag{50}$$

However, the requirement that equations (44) and (45) be satisfied is based on the assumption that equations (42) and (43) are used to specify how the Q space states are related to the P space states. As we can see from equations (35) and (36), alternative, more accurate expressions, which do *not* also require the eigenvalue criterion 50 to be satisfied are available, and should be used.

Thus, there are two distinct criteria. First, and more important, are the smallness of δ and $\mathbf{T}_Q^{-1}\delta \ll 1$,which guarantee that the solution of the CR equations entirely within the P space is an acceptable approximation to the P space part of the full solution. This is essential. The smallness of the P space eigenvalues in comparison to the Q space eigenvalues is required only to ensure that the initial Q space contribution (or Q space source term contribution) to the P space is given by $-\mathbf{H}\mathbf{M}_Q^{-1}$, and that the Q space densities in equilibrium with the P space states are given by $-\mathbf{M}_Q^{-1}\mathbf{V}$. If these expressions are replaced by $-\mathbf{\Delta}\mathbf{T}_Q^{-1}$ and $\delta\mathbf{T}_P^{-1}$ respectively, then there is no requirement on the relative sizes of the eigenvalues of M. Conversely, if a CR model with suitably small δ has been constructed, but for which the eigenvalue criterion fails, then $-\mathbf{\Delta}\mathbf{T}_Q^{-1}$ and $\delta\mathbf{T}_P^{-1}$ *must* be used for the population coefficients. Finally, if δ and $\mathbf{T}_Q^{-1}\delta \ll 1$ are not small, it is not possible to construct an adequate CR model, even if the eigenvalue criterion is satisfied. Notice, finally, that if indeed $\delta \ll 1$, then equation (36) implies that the Q space densities are all small in comparison to the P space densities.

3 Use of the code

Thus, any code which produces CR rates needs to specify:

1. The set of l species to be included in the calculation:
2. The 'bare' rate coefficients $\mathcal{R}_{i,j}^k(T)$ and Einstein A coefficients which couple all these l species:
3. The external source $\mathbf{\Gamma}$:
4. The locations and values of the fixed densities $N_1 \cdots N_K$:
5. The size of the P space and the species it contains, which also defines the size and content of the Q space.

and should give, on output at least:

1. The $l' \times l'$ coupling matrix $\mathbf{M}_{\text{eff}}$:

2. The population coefficients for the Q space states in equilibrium with the P space states, i.e., the matrix $\delta\mathbf{T}_P^{-1}$ and, for comparison, the traditional $-\mathbf{M}_Q^{-1}\mathbf{V}$:

3. The population coefficients for the P space states derived from the Q space sources, i.e., the matrix $-\mathbf{\Delta}\mathbf{T}_Q^{-1}$ and, for comparison, the traditional $-\mathbf{H}\mathbf{M}_Q^{-1}$:

4. The eigenvalues of $\mathbf{M}_{\text{eff}}$, $\mathbf{M}_Q$ and $\mathbf{M}$:

5. The eigenvectors of $\mathbf{M}$:

6. Estimates of the accuracy of the CR model based on the values of $||\delta||$ and $||\mathbf{T}_Q^{-1}\delta||$:

This is what `crmol` is supposed to do. I give a brief description of the code.

1. The set of l species included in the calculation. The code divides the species into 9 genera. These are:

	Type	No of members	Comments
1	Vibrational states	n_{vib}	Molecular electronic ground state
2	Explicit singlet	n_{ex}^S	Electronically excited molecular singlets
3	'Rydberg singlet'	n_{ryd}^S	Molecular 'Rydberg' singlets
4	Explicit triplet	n_{ex}^T	Electronically excited molecular triplets
5	'Rydberg triplet'	n_{ryd}^T	Molecular 'Rydberg' triplets
6	H_2^+	0 or 1	1 if molecules are included, otherwise 0
7	H^-	0 or 1	1 if H^- production included, 0 otherwise
8	Atomic states	n_{atom}	All neutral H atomic states (including $1s$)
9	Protons	1	Counted with atomic states (see **3** below)

The electronically excited molecular states are divided into 'explicit' and 'Rydberg' singlets and triplets. The ground state of H_2 is, of course $(1s)^2$, and the important low-lying excited states are usually of the form $^{2S+1}(1s, nl\lambda)$, where $(nl\lambda)$ specifies the orbital of the excited electron and S is the total electron spin. There are $n(n+1)/2$ distinct states of each symmetry[3], of which n are singly degenerate $l\sigma$ states and $(n-1)n/2$ are doubly degenerate $l\lambda$ states $(l > 0, \lambda = 1, 2, \cdots l)$. We have $0 \leq l \leq n-1$. 'Explicit' states are characterized by all four quantum numbers n, l, λ, S, whereas 'Rydberg' states are characterized by only n, S, that is, their full electronic structure is not resolved. The electronic ground state is further resolved into vibrational sublevels. At present, only the $n = 2$ states are resolved. They are

[3]Of course the ground state can have only singlet symmetry.

singlet	triplet
$^1B\Sigma$	$^3b\Sigma$
$^1EF\Sigma$	$^3a\Sigma$
$^1C\Pi$	$^3c\Pi$

Thus, $n_{\rm ex}^S = 3$ and $n_{\rm ex}^T = 3$.

2. The $l \times l$ matrix of bare rates. The bare rates are generated as follows:

1. The vibrationally resolved molecular electronic ground state rates. These are of two types:

   (a) Rates *not* involving neutral electronically excited molecular states. These are generated by the same code as is used for the molecular states in edge_code. (These include rates for vibrational transitions $\nu \rightarrow \nu'$, $\mathrm{H}_2(\nu) + \mathrm{e} \rightarrow \mathrm{H}_2^+ + \mathrm{e} + \mathrm{e}$, *etc*, see Appendix 1. describes these rates and further details can be found in Greenland & Reiter (1996)).

   Notice, however, that process 6 in Greenland & Reiter (1996)

   $$\mathrm{H}_2(X^1\Sigma_g)(v) + e \rightarrow \mathrm{H} + \mathrm{H} + e$$

   direct dissociation through electron collisions. In `crmol` it is considered to result from direct excitation of the three $n = 2$ triplet states. The $a\Sigma$ and $c\Pi$ states decay radiativly to the lower lying $b\Sigma$ state, which dissociates to H + H with a rate which I take to be 3×10^{14} s^{-1}.

   (b) Rates involving electronically excited neutral molecules. These are based on the Sawada-Fujimoto (1995) (SF) approximations, with the following modifications:

      i. $\mathrm{H}_2(B^1\Sigma_u)$ and $\mathrm{H}_2(C^1\Pi_u)$ excitation from the $\mathrm{H}_2(X^1\Sigma_g)(v)$ ground state. The SF rates are replaced by rates based on an average over the rates calculated by Celiberto and Janev (1995). Details were given elsewhere and are repeated here in Appendix 2. Note that radiative decays from these excited states can both redistribute the ground state vibrational distribution, and also lead to decay to the vibrational continuum of the ground state *i.e.* to dissociation as described in Stephens and Dalgarno (1972). Both processes are included.

      ii. Rates for the excitation of electronic states are given by SF, on the assumption that there is only one member of the vibrational manifold of the ground state. For cases where we use the SF rates we use this rate for *excitation* from each vibrational level. However, the SF rate for the corresponding *de-excitation* to the electronic ground state must be shared

amongst all the ground state vibrational levels. We assume each vibrational state gets an equal share so that, for excitation to an excited state H_2^*

$$\mathcal{R}(H_2(X^1\Sigma_g)(v) \rightarrow H_2^*) = \mathcal{R}_{SF}(H_2(\mathrm{gs}) \rightarrow H_2^*)$$

but for de-excitation from this state

$$\mathcal{R}(H_2(X^1\Sigma_g)(v) \leftarrow H_2^*) = \frac{1}{n_{\mathrm{vib}}}\mathcal{R}_{SF}(H_2(\mathrm{gs}) \leftarrow H_2^*)$$

where $\mathcal{R}$ is the rate used in the code and $\mathcal{R}_{SF}$ is the SF rate.

2. Rates for dissociative recombination, dissociative attachment, etc. are calculated as in edge_code.

3. All other rates, including the atomic rates, are from SF, *but* SF add a term to the ionization rate $H_2^* \rightarrow H_2^+$ which represents an 'autoionization' channel. There is some doubt about what cross section they use to model this. At present (8-12-98) we use the Janev rate 11. The Janev rate 26 *may* be the appropriate one to use; more information will be available soon.

The non-zero elements of the coupling matrix **M** are then written out on stream 48[4] in the form $i; j, M_{i,j}$.

3. The ordering of the states. In much of what follows, the ordering of the states is important. The initial ordering is:

1. n_{vib} vibrational levels of the $H_2(X^1\Sigma_g)(v)$ state $v = 0 \cdots n_{\mathrm{vib}} - 1$ (indexed $1 \cdots n_{\mathrm{vib}}$.)

2. n_{ex}^S explicitly identified singlet states, indexed $n_{\mathrm{vib}} + 1 \cdots n_{\mathrm{vib}} + n_{\mathrm{ex}}^S$

3. n_{ryd}^S Rydberg singlet states, indexed $n_{\mathrm{vib}} + n_{\mathrm{ex}}^S + 1 \cdots n_{\mathrm{vib}} + n_{\mathrm{ex}}^S + n_{\mathrm{ryd}}^S$

4. n_{ex}^T explicitly identified triplet states, indexed $n_{\mathrm{vib}} + n_{\mathrm{ex}}^S + n_{\mathrm{ryd}}^S + 1 \cdots n_{\mathrm{vib}} + n_{\mathrm{ex}}^S + n_{\mathrm{ryd}}^S + n_{\mathrm{ex}}^T$

5. n_{ryd}^T Rydberg triplet states, indexed $n_{\mathrm{vib}} + n_{\mathrm{ex}}^S + n_{\mathrm{ryd}}^S + n_{\mathrm{ex}}^T + 1 \cdots n_{\mathrm{vib}} + n_{\mathrm{ex}}^S + n_{\mathrm{ryd}}^S + n_{\mathrm{ex}}^T + n_{\mathrm{ryd}}^T$

6. 1 H_2^+ state indexed $n_{\mathrm{vib}} + n_{\mathrm{ex}}^S + n_{\mathrm{ryd}}^S + n_{\mathrm{ex}}^T + n_{\mathrm{ryd}}^T + 1$

7. **If there is a channel for H^- production,** 1 H^- state indexed $n_{\mathrm{vib}} + n_{\mathrm{ex}}^S + n_{\mathrm{ryd}}^S + n_{\mathrm{ex}}^T + n_{\mathrm{ryd}}^T + 2$. This state is *absent* if there is no H^- production mechanism. Thus we can define

$$n_{\mathrm{mol}} = n_{\mathrm{vib}} + n_{\mathrm{ex}}^S + n_{\mathrm{ryd}}^S + n_{\mathrm{ex}}^T + n_{\mathrm{ryd}}^T + 2$$

[4]In all cases stream n is associated with the file `fort.n`.

if H^- is produced,

$$n_{\rm mol} = n_{\rm vib} + n^S_{\rm ex} + n^S_{\rm ryd} + n^T_{\rm ex} + n^T_{\rm ryd} + 1$$

if H^- is *not* produced.

If there are no vibrational levels specified *ie* if $n_{\rm vib} \leq 0$, then none of the above is relevant and the code sets $n_{\rm mol} = 0$, which enables a CR model in the absence of molecules to be constructed.

8. The atomic H ground state. This has index $n_{\rm mol} + 1$
9. The protons with index $n_{\rm mol} + 2$
10. $n_{\rm atom} - 1$ atomic excited states, with index $n_{\rm mol} + 3 \cdots n_{\rm mol} + n_{\rm atom} + 1$.

Important details of the enumeration are given on stream 21. An example is shown here. Initially, 15 vibrational sublevels of the ground state, 3 explicit singlet and 10 Rydberg singlet states, 3 explicit triplet and 10 Rydberg triplet states, H_2^+, H^- and 10 atomic states were considered. This gives a total of 15+3+10+3+10+1+1+10=53 states. In addition to the electron density, the proton density was also held fixed, so that species 45 is removed from subsequent manipulations. The remaining 52 states are permuted so that the first 18 (in this case — see below), the 15 vibrational levels of the ground state, H_2^+, H^- and H($1s$) are in the P space. Their final designation, and initial location are then listed.

First, the simple listing of the initial states and their indicies. The specification of the states is supposed to be self explanatory.

```
GS v=  0   1
GS v=  1   2
GS v=  2   3
GS v=  3   4
GS v=  4   5
GS v=  5   6
GS v=  6   7
GS v=  7   8
GS v=  8   9
GS v=  9  10
GS v= 10  11
GS v= 11  12
GS v= 12  13
GS v= 13  14
GS v= 14  15
esing  1  16
esing  2  17
```

```
esing  3  18
rsing  1  19
rsing  2  20
rsing  3  21
rsing  4  22
rsing  5  23
rsing  6  24
rsing  7  25
rsing  8  26
rsing  9  27
rsing 10  28
etrip  1  29
etrip  2  30
etrip  3  31
rtrip  1  32
rtrip  2  33
rtrip  3  34
rtrip  4  35
rtrip  5  36
rtrip  6  37
rtrip  7  38
rtrip  8  39
rtrip  9  40
rtrip 10  41
H2+    1  42
H-        43
H(1s)     44
H+        45
H(n)=  2  46
H(n)=  3  47
H(n)=  4  48
H(n)=  5  49
H(n)=  6  50
H(n)=  7  51
H(n)=  8  52
H(n)=  9  53
esing 1 is Bsigma
esing 2 is EFsigma
esing 3 is Cpi
etrip 1 is bsigma
etrip 2 is asigma
etrip 3 is cpi
```

followed by a reminder for later

```
NB in fort.98 and fort.99 the electronically excited states
of the molecule are labelled 1,2 ...N_max=n_explicit+n_rydberg+1
2,3,4 are the explicit states above (S=singlet, T=triplet)
5 .... N_max are the singlet (S) or triplet (T) Rydberg states
and state 1 (S or T) is always the electronic ground state,
which is given honourary triplet status for the purpose of
electronic collisions and radiative recombination
N/A means not applicable - rates so labelled are not used
```

and details of fixed densities.

```
density fixed for H+         45
```

Now, the final state ordering, showing the position in the final state vector of the explicitly identified state and its original index before any modifications (including the fixing of densities) were made.

```
The re-ordered matrix labels
final state          1 is GS v=  0   1
final state          2 is GS v=  1   2
final state          3 is GS v=  2   3
final state          4 is GS v=  3   4
final state          5 is GS v=  4   5
final state          6 is GS v=  5   6
final state          7 is GS v=  6   7
final state          8 is GS v=  7   8
final state          9 is GS v=  8   9
final state         10 is GS v=  9  10
final state         11 is GS v= 10  11
final state         12 is GS v= 11  12
final state         13 is GS v= 12  13
final state         14 is GS v= 13  14
final state         15 is GS v= 14  15
final state         16 is H2+    1  42
final state         17 is H-        43
final state         18 is H(1s)     44
final state         19 is rsing  1  19
final state         20 is rsing  2  20
final state         21 is rsing  3  21
final state         22 is rsing  4  22
final state         23 is rsing  5  23
final state         24 is rsing  6  24
final state         25 is rsing  7  25
```

```
final state        26 is rsing  8  26
final state        27 is rsing  9  27
final state        28 is rsing 10  28
final state        29 is etrip  1  29
final state        30 is etrip  2  30
final state        31 is etrip  3  31
final state        32 is rtrip  1  32
final state        33 is rtrip  2  33
final state        34 is rtrip  3  34
final state        35 is rtrip  4  35
final state        36 is rtrip  5  36
final state        37 is rtrip  6  37
final state        38 is rtrip  7  38
final state        39 is rtrip  8  39
final state        40 is rtrip  9  40
final state        41 is rtrip 10  41
final state        42 is esing  1  16
final state        43 is esing  2  17
final state        44 is esing  3  18
final state        45 is H(n)=  2  46
final state        46 is H(n)=  3  47
final state        47 is H(n)=  4  48
final state        48 is H(n)=  5  49
final state        49 is H(n)=  6  50
final state        50 is H(n)=  7  51
final state        51 is H(n)=  8  52
final state        52 is H(n)=  9  53
```

4. The fixed densities. This indexing identifies the species. It is assumed that the electron density is fixed. If no other species is to be set at a fixed density, the CR model can be constructed (see below). If the densities of certain species are to be explicitly fixed, then their index, and the value of their density is specified, and the new effective matrix $\mathbf{M}$ and $\mathbf{\Gamma}_{\rm CR}$ are constructed, by removing entries in the matrix corresponding to the fixed densities, and constructing the corresponding source term $\mathbf{\Gamma}_{\rm CR}$.

NOTE *The proceedure used only produces the component of the source term which corresponds to the interaction between explicitly fixed species and electrons. It fails to include the component which corresponds to the interactions of the explicitly fixed species amongst themselves.*

Two further points must be noticed:

1. The original indexing is described in **3** above. This will be modified, since each fixed species is considered to be removed from the original

matrix, to produce the effective matrix. For example, in the original matrix, the protons have index $n_{\rm mol}+2$ (45 in the example), and the 1st atomic H excited state has index $n_{\rm mol}+3$ (46 in the example). If the proton density is fixed, protons disapear from the list of species, and all species whose index was originally greater than $n_{\rm mol}+2$ have their index reduced by 1 so that the 1st atomic H excited state will have index $n_{\rm mol}+2$ in the effective matrix, not $n_{\rm mol}+3$, as it had in the original matrix. These modified indicies must be used on stream 7, to specify the P space.

2. Processes which cannot be included without violating linearity are automatically excluded by the program. For example, collisions involving electrons and H^- are in order. However collisions involving protons and H^- lead to non-linear terms in 1, unless *eg* the proton density is fixed. The code automatically excludes the contribution of $p-H^-$ collisions (even if it is included in the original set of reactions) unless the proton (or H^-) density is specified as fixed.

5. The P space. The number of states in the P space N_P and their location according to the indexing described above must be given. The code then permutes the matrix $\mathbf{M}$, $\mathbf{n}$ and $\mathbf{\Gamma}_{\rm CR}$ so that the P space states occur first in $\mathbf{n}$ and $\mathbf{\Gamma}_{\rm CR}$, and the P space couplings are in the top left corner of M. The CR matrix $\mathbf{M}_{\rm eff}$ the source term $\mathbf{\Gamma}_P$ (eqns 8 and 10) and $\mathbf{M}_Q^{-1}\mathbf{V}$ are then constructed[5]. At this stage the following is output:

stream 48 $j,i,\mathrm{M}(j,i)$, the full matrix, before removal of the fixed densities.

stream 49 $j,i,\mathrm{M}(j,i)$ after removal of fixed densities, in its original order.

stream 12 $j,i,\mathrm{M}(j,i)$ after removal of fixed densities, and permutation to isolate the P space

stream 25 $i,\Gamma_{\rm CR}(i)$ in its permuted order

stream 22 $j,i,\mathrm{M}_{\rm eff}(j,i)$ for use in the CR model

stream 23 $i,\Gamma_{\rm P}(i)$ for use in the CR model

stream 32 $j,i,\mathrm{M}_Q(j,i)$ for use in the CR model

stream 33 $j,i,\left[\mathbf{M}_Q^{-1}\mathbf{V}\right](j,i)$

stream 34 $j,i,\left[\delta\mathbf{T}_P^{-1}\right](j,i)$

stream 35 $j,i,\left[\mathbf{H}\mathbf{M}_Q^{-1}\right](j,i)$

[5]See appendix 4 for a complete list of streams in numerical order.

stream 36 $j, i, \left[\Delta \mathbf{T}_Q^{-1}\right](j,i)$

stream 80 $j, i, \mathbf{V}(j,i), \mathbf{H}(i,j)$

stream 81 $j, i, \mathbf{M}_Q^{-1}(j,i)$

stream 21 First, details of the state enumeration and permutation, as described above, followed by $l - K$ lines of the form i, x, y, a, b, e where:

- i is a running index
- x is the ith eigenvalues of the full matrix $\mathbf{M}$
- y is the ith eigenvalue of $\mathbf{M}_{\text{eff}}$ if $i \leq N_P$
- y is the $i - N_P$th eigenvalue of $\mathbf{M}_Q$ if $i > N_P$
- a is the ith component of the nevx'th eigenvector of $\mathbf{M}$ (see input for definition of nevx).
- b is the ith component of the nevx'th eigenvector of $\mathbf{M}_{\text{eff}}$ for $i \leq N_P$. If nevx $> N_P$, this column is zero. $b = 0$ if $i > N_P$.
- e is the error associated with the ith P state.$(1 \leq i \leq N_P)$ or $i - N_P$th Q state $(N_P + 1 \leq i \leq N_P + N_Q)$. For the P states the error given is $\epsilon_{\text{tot}}^{(i)}$; for the Q states $\epsilon_4^{(i-N_P)}$ is given (see section 5).

stream 99 All the non-zero individual rates used in the code are written out and identified both by a brief description and an index k. Those marked N/A are not used. However, some rates involving H_2^+ and H^- are calculated and written out to streams 90, 99 and 98 (see section 4) whether or not H_2^+ or H^- is present in the calculation. They are, of course, not used for calculations without H_2^+ or H^-. THe matrix indices in stream 90 will then not correspond to valid locations.

stream 90 Gives similar details to stream 99, but in the form i, j, k, R, q, where the k'th rate with value R contributes to $\mathbf{M}_{ij}$ and corresponds to a process which gives q nuclei. If the matrix indices do not correspond to a valid location, the rate is not used in the calculation (see above).

This is the main output from the part of the code which calculates CR rates. Outputs on streams 60, 61, 78, 79, 77, 45, 51, 98 and 95, which are connected with the energy rates, are described in section 4, and output on streams 87, 93 and 94 which deal with the accuracy of the model is described in section 5. Some diagnostic output is also produced.

stream 17 N, N_P fullowed by N rows of the form i, ipq(i), ipqf(i), where i is the final index in $\mathbf{M}$, ipq(i) the original index (after removal of fixed densities, but before permutation to isolate the P space), and ipqf(i) is the original index after permutation; i e the state at i in

M corresponds to the species with original label ipqf(i), as listed on stream 21. index, ipq(i) is

stream 47 i, isn(i), where i is the *original* species index, and isn(i) = 0 if state i is kept in the final matrix, isn(i) = 1 state i is removed. This information is written twice, omce from the rate calculation, once from the energy rate calculation.

stream 70 i, colsum(i), sn(i), where colsum(i) = $\sum_j K(j)M_{j,i}$, with $K(j)$= number of nuclei in species j, and sn(i) = $\sqrt{\sum_j M_{j,i}^2}$. If colsum(i)/sn(i) > 10^{-14} a diagnostic message is also written on stdout. This is only relevant if no heavy particle densities are fixed.

stream 91 i, e_i, f_i, where e_i is the real part, and f_i the imaginary part of the i'th eigenvalue of the *permuted*[6] matrix M. The eigenvalues are arranged in order of increasing absolute value, and the corresponding eigenvectors are written on stream 93 (see section 5).

stream 92 is identical to stream 91, except that the eigenvectors are those of the *unpermuted ie* the states are in their *original* order *cf* stream 49. The corresponding eigenvectors are on stream 94 (see section 5).

stream 96 The non-zero elements of the permutation matrix which operates on the original ordering of states to give the final ordering.

stream 97 Data on the singlet-triplet rates
$j, i, C_{st}(i,j), F_{st}(i,j), C_{ts}(j,i), F_{ts}(j,i), \Delta E, j_s, i_t$, where:

i is the triplet index, j is the singlet index

$C_{st}(i,j)$ is the excitation rate coefficient from the singlet state labelled by j to the triplet state labelled by i

$F_{st}(i,j)$ is the de-excitation rate coefficient from the singlet state labelled by j to the triplet state labelled by i

$C_{ts}(j,i)$ is the excitation rate coefficient from the triplet state labelled by i to the singlet state labelled by j

$F_{ts}(j,i)$ is the de-excitation rate coefficient from the triplet state labelled by i to the singlet state labelled by j

ΔE = (Binding energy of triplet state i_t − Binding energy of singlet state j_s)

j_s, i_t, indices for the singlet and triplet binding energies

stream 97 is not written if stf=0.

[6] *ie* the states are in their *final* order *cf* stream 12.

The input to get this is on stdin and stream 7. On stdin it is of the form:

```
ifrgn nev
nvv nsexp nsryd ntexp ntryd natom
temp densel nproc (ipick(k+3),k=1,nproc)
nfix (locfix(k),k=1,nfix),(denfix(k),k=1,nfix)
nres
iflg yman
nfix (locfix(i),i=1,nfix),(denfix(i),i=1,nfix)
forwrd back
stf
nps nev
```

and on stream 7 it is of the form

```
ip(k),k=1,nps
```

The meaning of the input is described below. In general it is a straightforward reflection of the above discussion, but the following should be noted

1. `nproc,(ipick(k+3),k=1,nproc)`. This is similar, but not identical to the input to edge_code, described in Greenland & Reiter (1996) and the supplement *'How to run the Edge Code'* (24 April 1997). A summary is appended in Appendix 1. The main changes reflect the exsplicit treatment of the $n = 2$ states. `iproc(k),k=1,3` are hard wired as processes 1, 2 and 10 *ie* electron impact excitation of ground state vibrational levels (1 and 2) and electron impact ionization of H_2 to H_2^+ (10), (see Appendix 1) Furthermore, process 6, electron impact dissociation, is now included as direct electron impact excitation of the $^3b\Sigma$ state, whose rate coefficients are discussed in Appendix 3. Thus, if processes 1, 2, 6 or 10 are specified in `ipick` the code writes a warning that they will lead to double counting, which indeed they will. Specifying `nproc=0` is legal, and leads to the automatic inclusion of electron impact vibrational excitation, electron impact ionization and electron impact dissociation through the $^3b\Sigma$ state of H_2.

2. `iflg` is used to select which molecular electronic ground state to electronic $n = 2$ excited states are used. If `iflg` ≥ 0 the data described here are used. If `iflg` < 0, two choices, based on the SF data, are available. They vary in their treatment of radiative transitions from the $n = 2$ molecular states to the ground state. Some SF calculations replace the 15 vibrational levels of the H_2 electronic ground state with an 'effective' molecular ground state, and the radiative rates for transitions to this 'effective' state are what is included in the SF data. Setting `iflg` ≤ -10

(and nvv = 1) reproduces this stratagy. If $-9 \leq$ iflg ≤ -1, it is assumed that the 15 vibrational levels are resolved and that the SF radiative decay rates from $n = 2$ are equally distributed amongst all 15 vibrational levels, so that the decay rate to each level = $1/15\times${the SF $n = 2 \rightarrow$ gs rate}. This is only fully consistent if nvv = 15.

3. nfix (locfix(k),k=1,nfix),(denfix(k),k=1,nfix) is used to set the number and location of the fixed densities. The electron density is always assumed to be fixed, and if it is the only fixed density then nfix=0 should be set. (nfix=-1 is no longer legal). Otherwise, set nfix to the number of fixed densities (excluding the electron density), and set locfix and denfix to the locations and values of the fixed densities in the matrix. **WARNING:** *If* nfix *is greater than 1, the source term* $\mathbf{\Gamma}_{\rm CR}$ *will* **ONLY** *be set correctly if there is* **NO** *interaction between those species, other than electrons, whose densities are fixed. This will be corrected later.*

4. forward and back enable the $pH^- \rightarrow H(H^*) + H$, and Ion Conversion rates (including the rates for the inverse processes, if they are active) respectivly to be multiplied by these factors. The standard values are both unity.

5. stf is the 'singlt-triplet fudge factor'. There is no data for electron impact induced transitions between electronically excited molecular singlet and triplet states. A crude approximation, which enables the effects of such transitions to be examined, is included in the code. It uses the Janev(1987) rate 2.3.4d $He(1s2p|^3P) \rightarrow He(1s2p|^1P)$ as typical, and the effective molecular singlet-triplet energies to distinguish between excitation and de-excitation, and to relate these rates by detailed balance. The rates used in the code are then all multiplied by stf, which should be non-negative. stf = 0 removes the singlet-triplet coupling.

6. nev specifies the eigenvector to be written on stream 21. If nev ≥ 1 then nevx = nev. If nev< 0 nevx = nerr, where nerr ($1 \leq$ nerr $\leq N_P$) is the index of the eigenvector with maximum error $\epsilon_{\rm tot}^{\rm (nerr)}$ (see section 5). If $1 \leq$ nevx $\leq N_P$ the eigenvectors of both $\mathbf{M}$ and $\mathbf{M}_{\rm eff}$ are written out. If $N_P + 1 \leq$ nevx $\leq N$ only the eigenvector of $\mathbf{M}$ is written.

Further details are documented in the code itself.

The input data have the following meaning and restrictions. Bold faced values are mandatory. Values in brackets are recommended.

stdin

ifrgn	=	negative integer (see section 5)
nev	=	not used here (see section 5)
nvv	=	$n_{\rm vib} \leq 15$
nsexp	=	$n_{\rm ex}^S = \mathbf{3}$
nsryd	=	$n_{\rm ryd}^S \leq 37$
ntexp	=	$n_{\rm ex}^T = \mathbf{3}$
ntryd	=	$n_{\rm ryd}^T \leq 37$
natom	=	$n_{\rm atom} \leq 40$
temp	=	temperature (eV)
densel	=	electron density ($\rm cm^{-3}$)
nproc	=	number of molecular processes
iproc(k+3),k=1,nproc	=	indices for molecular processes (see 1. above)
nres	=	Principal quantum number of highest resolved electronic state =2
iflg	=	Flag ≥ 0 use data described here, < 0 see 3. above
yman	=	=1 for optically thin H($2p$) state, = 0 for optically thick H($2p$) state
nfix	=	number of explicit fixed densities
locfix(k),k=1,nfix	=	indices for fixed densities
denfix(k),k=1,nfix	=	values for fixed densities ($\rm cm^{-3}$)
forward	=	factor for H^- charge transfer ($p + H^- \rightarrow H + H^{(*)}$) (=1)
back	=	factor for Ion Conversion ($H_2 + p \rightarrow H_2^+ + H$) (=1)
stf	=	singlet triplet fudge factor (≥ 0) — see 7. above
nps	=	N_P
nev	=	index number of eigenvector to be written on stream 21 (see above)

stream 7

(ip(k),k=1,nps) = locations of P space states before permutation

These should be given in increasing order, so that ip(k) < ip(k+1), k=1,nps-1.

Finally, the following stop codes are used

1. STOP 100 — Error in Foreign Matrix (only relevant if ifrng.gt.0),
2. STOP 999 — correct exit for processing a Foreign Matrix (only relevant if ifrng.gt.0),
3. STOP 666 — subroutine diag has attempted to diagonalize a matrix with dimension less than 1,
4. STOP 9 — subroutine revmat has detected an error while creating M.

4 Electron energy loss rates.

We can construct a set of electron energy rate coefficients $\mathcal{S}_j^k(T)$ in exact analogy to $\mathcal{R}_j^k(T)$ where $\mathcal{R}_j^k(T)$ is the usual rare coefficient for the electron induced process $k \leftarrow j$ at electron temperature T. For electrons of speed $v \rightarrow v + dv$ we have

$$\frac{d\dot{\epsilon}_j^k}{dv} dv = n_j N_e f_T(v) v \Delta_j^k(v) \sigma_j^k(v) dv \tag{51}$$

where $d\dot{\epsilon}_j^k/dv$ is the rate of energy delivery/unit volume to the electrons due to collisions of those electrons in the speed range $v \rightarrow v + dv$ which induce the process $k \leftarrow j$. $\Delta_j^k(v)$ is the explicit energy loss experienced by these electrons, and $\sigma_j^k(v)$ is the cross section for the process $k \leftarrow j$. $f_T(v)dv$ is the electron speed distribution at temperature T, which we take to be a Maxwell Boltzmann distribution.

Integrating 51 over electron velocity gives

$$\dot{\epsilon}_j^k = n_j N_e \int f_T(v) v \Delta_j^k(v) \sigma_j^k(v) dv \tag{52}$$

which enables us to define

$$\mathcal{S}_j^k(T) = \int f_T(v) v \Delta_j^k(v) \sigma_j^k(v) dv \tag{53}$$

and to write, in analogy to equation 15

$$\dot{\mathcal{E}} = \mathbf{U}(N_1 \cdots N_K)\mathbf{n} + \Xi_{\mathrm{E}}(N_1 \cdots N_K) \tag{54}$$

where

$$\dot{\mathcal{E}}_k = \sum_j \dot{\epsilon}_j^k \tag{55}$$

is the total rate of electron energy loss/unit volume implied by the production of species k from electron collisions with all other species j,

$$U_{k,j} = \mathcal{S}_j^k(T) N_e \tag{56}$$

is the energy loss rate matrix, the analogue of $M_{k,j}(T)$ discussed in section 2 and

$$\Xi_{\mathrm{E,k}} = \sum_i \mathcal{S}_i^k N_i N_e \tag{57}$$

is the electron energy sink derived from electron collisions with the fixed density species N_i. Notice that this treatment only includes electron energy changes which result from electron collisions with other species. Processes such as

$$\mathrm{H}^- + \mathrm{p} \rightarrow \mathrm{H} + \mathrm{p} + \mathrm{e}$$

which make a contribution to the electron energy budget, but which require a knowledge of the proton velocity distribution for their calculation are excluded. `crmol` identifies such processes as 'TOO DIFFICULT' and sets their rate to zero.

The CR approximation described above can be used to write (the CR approximation to) equation 54 as

$$\begin{bmatrix} \dot{\mathcal{E}}_1 \\ \dot{\mathcal{E}}_2 \\ \vdots \\ \dot{\mathcal{E}}_k \\ \vdots \end{bmatrix} = \begin{bmatrix} \mathbf{U}_P - \mathbf{U}_H\mathbf{M}_Q^{-1}\mathbf{V} \\ \mathbf{U}_V - \mathbf{U}_Q\mathbf{M}_Q^{-1}\mathbf{V} \end{bmatrix} \begin{bmatrix} n_{P,1} \\ n_{P,2} \\ \vdots \end{bmatrix} + \begin{bmatrix} \Xi_{E,1} \\ \Xi_{E,2} \\ \vdots \\ \Xi_{E,k} \\ \vdots \end{bmatrix} \tag{58}$$

where, of course, in complete analogy to equation 19, we have

$$\begin{bmatrix} \dot{\mathcal{E}}_1 \\ \dot{\mathcal{E}}_2 \\ \vdots \\ \dot{\mathcal{E}}_k \\ \vdots \end{bmatrix} = [\mathbf{U}_{\text{eff}}] \begin{bmatrix} n_{P,1} \\ n_{P,2} \\ \vdots \end{bmatrix} + \begin{bmatrix} \Xi_{E,1} \\ \Xi_{E,2} \\ \vdots \\ \Xi_{E,k} \\ \vdots \end{bmatrix} \tag{59}$$

with

$$\mathbf{U} = \begin{bmatrix} \mathbf{U}_P & \mathbf{U}_H \\ \mathbf{U}_V & \mathbf{U}_Q \end{bmatrix} \tag{60}$$

Notice that, unlike the CR population equations, which involve $l' \times l'$ matrices these expressions involve $l \times l'$ matrices. This expresses the fact that the rate of electron *energy loss* associated with the small populations of Q space species is not required to be small. In contrast, the rate of *population* change of the Q space species is small.

In order to calculate $\mathcal{S}_j^k$ we need expressions for $\Delta_j^k(v)$, the electron *energy loss* due to the collision $k \leftarrow j$. There are five cases:

1. Electron induced transitions between bound states. Here

$$\Delta_j^k(v) = E_k - E_j \tag{61}$$

so that

$$\mathcal{S}_j^k = (E_k - E_j)\mathcal{R}_j^k \tag{62}$$

where E_k is the final state energy and E_j the initial state energy (negative for bound states).

2. Electron induced ionization of bound states. Since we are only interested in the total change in electron energy, irrespective of how the electron density varies we have

$$\Delta_j^k(v) = -E_j \tag{63}$$

so that

$$\mathcal{S}_j^k = -E_j \mathcal{R}_j^k \tag{64}$$

where E_j the initial state energy (negative for bound states).

3. Three body recombination. In exact analogy to case 2, above,

$$\Delta_j^k(v) = E_k \tag{65}$$

so that

$$\mathcal{S}_j^k = E_k \mathcal{R}_j^k \tag{66}$$

where E_k the energy of the final state occupied by the captured electron (negative for bound states).

4. Radiative and dissosiative recombination and attachment. Here

$$\Delta_j^k(v) = \frac{1}{2} m v^2 \tag{67}$$

where m is the electron mass. Once again I stress that this is the energy removed from the electron sea. Notice it does not depend on the final state into which the electron is captured. It is straightforward to show that

$$\mathcal{S}_j^k = \frac{3}{2} T \mathcal{R}_j^k - \frac{\partial \mathcal{R}_j^k(\beta)}{\partial \beta} \tag{68}$$

where $\beta = 1/T$. Explicit expressions are given in appendix 1.

5. Electron induced dissociation. For processes such as

$$\mathrm{e} + \mathrm{H}_2(\nu) \rightarrow \mathrm{e} + \mathrm{H} + \mathrm{H}$$

$$\Delta_j^k(v) = K - E_j \tag{69}$$

where K is the total energy of the fragments, and E_j is the energy of the initial state. However K is not fixed; its distribution $P(K, v)$ depends upon the electron impact velocity, and we must average Δ_j^k over this distribution. We may write

$$P(K, v) dK = \frac{d\sigma(K, v)}{dK} / \sigma(v) dK \tag{70}$$

where

$$\frac{d\sigma(K, v)}{dK}$$

is the cross section for dissociation, differential in heavy particle kinetic energy. This can often be obtained from the appropriate bound-free Franck-Condon factor. Using 70 in 53 gives

$$\mathcal{S}_j^k = \int dv f_T(v) v \int dK K \frac{d\sigma(K,v)}{dK} - E_j \mathcal{R}_j^k \tag{71}$$

where E_j the initial state energy (negative for bound states).

Notice that, provided the Franck-Condon principle applies to the dissociative transition, the first term in equation 70 can be written

$$\int dv f_T(v) v \int dK K \frac{d\sigma(K,v)}{dK} = \int dv f_T(v) v \sigma(v) \bar{K}_j = \mathcal{R}_j^k \bar{K}_j \tag{72}$$

with

$$\bar{K}(v) = \int dK K q_{K,j} \tag{73}$$

where $q_{K,j}$ is the bound-free Franck-Condon factor for the dissociative transition from initial state j. Thus $\bar{K}_j$ is the mean kinetic energy of the fragments.

In many cases Janev *et al* give values for $\bar{K}_j - E_j$, where j represents the ground vibrational state of the molecule, and as an interim measure I use these values, corrected by the vibrational excitation energy as appropriate. This approximation will be improved. However, its use does enable estimates of the electron energy loss to be made. The output is as follows:

stream 60 $i, j, \mathbf{U}_{\text{eff}}(i,j)$, the effective $l \times l'$ energy rate matrix. See equation 58 *etc.*

stream 61 $j, \sum_i \mathbf{U}_{\text{eff}}(i,j), \bar{E}(j) = -\sum_i \mathbf{U}_{\text{eff}}(i,j)/\mathbf{M}_{\text{eff}}(j,j)$, the effective total electron energy loss rate/P space species

stream 78 $j, i, \bar{E}(j,i), \mathbf{U}(j,i), \mathbf{M}(j,i)$ $\mathbf{U}$ (equation 54) is the analogue of $\mathbf{M}$, (equation 13). $\bar{E}(j,i) = \mathbf{U}(j,i)/\mathbf{M}(j,i)$ is the mean electron loss associated with the process $j \leftarrow i$.

stream 79 $i, \bar{E}_i, \Xi_E(i), \Gamma(i)$ in the permuted order. $\bar{E}_i = \Xi_E(i)/\Gamma(i)$ is the mean electron energy loss associated with the source i.

stream 77 $j, \bar{E}(j), \sum_i \mathbf{U}(i,j), -\mathbf{M}(j,j)$ with $\bar{E}(j) = -\sum_i \mathbf{U}(i,j)/\mathbf{M}(j,j)$, the effective total electron energy loss rate/species

stream 45 The energy rate matrix in the original order; (the analogue of stream 48).

stream 51 The energy rate matrix after the removal of the fixed densities; (the analogue of stream 49).

stream 95 This is the exact analogue of stream 97, but dispalys the singlet-triplet energy rates. It is not written if `stf=0`.

stream 98 The individual energy loss rates, the analogue of stream 99 in the form $\bar{E}_{k,j}$,<index>,$\mathcal{S}_j^k$, <description>, where $\bar{E}_{k,j} = \mathcal{S}_j^k/\mathcal{R}_j^k$ is the mean electron energy loss/process.

5 Accuracy Considerations

In summary, in section 2 I have described the criteria for the accuracy of the CR model. They are

$$\left.\begin{array}{r} \delta \ll 1 \\ \mathbf{T}_Q^{-1}\delta \ll 1 \end{array}\right\} \qquad \text{A}$$

$$|\lambda^{(k_P)}| < |\lambda^{(k_Q)}| \;\; 1 \le k_P \le N_P; \;\; N_P + 1 \le k_Q \le N \qquad \text{B}$$

$$|\lambda^{(N_P)}| \ll |\lambda^{(N_P+1)}| \qquad \text{C}$$

These satisfaction of these criteria guarentees:

A $\mathbf{M}_{\text{eff}}$ adaquately describes the motion of the P space states

B The Q space states decay faster than the P space states

C This is not strictly necessary, but if it is fulfilled, then the population coefficients are adequately given by $-\mathbf{M}_Q^{-1}\mathbf{V}$ and $-\mathbf{H}\mathbf{M}_Q^{-1}$. This is elaborated below.

Using the the l_1 (Manhatten) norm $||\mathbf{v}||_1$ *viz*

$$||\mathbf{v}||_1 = \sum_{k=1}^{n} |v_k| \tag{74}$$

I can define

$$\epsilon_1^{(k)} = \sum_{j=1}^{N_Q} |\delta_{jk}| \;\; k = 1 \cdots N_P \tag{75}$$

$$\epsilon_2^{(k)} = \sum_{j=1}^{N_Q} |\left[\mathbf{T}_Q^{-1}\delta\right]_{jk}| \;\; k = 1 \cdots N_P \tag{76}$$

$$n_1^{(k)} = \sum_{j=1}^{N_Q} |\left[\delta\mathbf{T}_P^{-1} + \mathbf{M}_Q^{-1}\mathbf{V}\right]_{jk}| \;\; k = 1 \cdots N_P \tag{77}$$

$$d_1^{(k)} = \sum_{j=1}^{N_Q} | \left[\mathbf{M}_Q^{-1} \mathbf{V} \right]_{jk} | \quad k = 1 \cdots N_P \tag{78}$$

$$\epsilon_3^{(k)} = \begin{cases} n_1^{(k)} / d_1^{(k)} & d_1^{(k)} \neq 0 \\ n_1^{(k)} & d_1^{(k)} = 0 \end{cases} \quad k = 1 \cdots N_P \tag{79}$$

and

$$\epsilon_{\text{tot}}^{(k)} = \epsilon_1^{(k)} + \epsilon_2^{(k)} \tag{80}$$

Thus, $\epsilon_{\text{tot}}^{(k)}$ gives some estimate of the total error associated with the k'th P space state. Similarly, we have

$$n_2^{(k)} = \sum_{j=1}^{N_P} | \left[\mathbf{\Delta T}_Q^{-1} - \mathbf{H} \mathbf{M}_Q^{-1} \right]_{jk} | \quad k = 1 \cdots N_Q \tag{81}$$

$$d_2^{(k)} = \sum_{j=1}^{N_P} | \left[\mathbf{H} \mathbf{M}_Q^{-1} \right]_{jk} | \quad k = 1 \cdots N_Q \tag{82}$$

$$\epsilon_4^{(k)} = \begin{cases} n_2^{(k)} / d_2^{(k)} & d_2^{(k)} \neq 0 \\ n_2^{(k)} & d_2^{(k)} = 0 \end{cases} \quad k = 1 \cdots N_Q \tag{83}$$

so that $\epsilon_3^{(k)}$ and $\epsilon_4^{(k)}$ represents the error associated with the use of the conventional population coefficients.

The accuracy data, summarized on stream 21, is written out in greater detail on stream 87 *viz*:

stream 87 Three sets of data, separated by blank lines are written

$i, \epsilon_1^{(i)}, \epsilon_2^{(i)}, \epsilon_3^{(i)}, d_1^{(i)}$, where i runs from $1 \rightarrow N_P$.

blank line

$i, \epsilon_4^{(i)}, d_2^{(i)}$, where i runs from $1 \rightarrow N_Q$.

blank line

$\texttt{nerr}, \epsilon_{tot}^{(\text{nerr})}$

Finally, we may note that this analysis of the CR model has three consequences, which we list here, but discuss more fully elsewhere.

1. The requirement that δ must be small, coupled with the requirement that the the eigenvalues must be ordered can be used to construct an algorithm which automatically identifies the P space states.

2. The ordering of the eigenvalues enables the limit 32 to be taken consistently, and thus leads to 34. However, this does not imply that all the components of $\mathbf{E}t$ (31) are non-negligible. It is possible — indeed in most cases with molecules probable — that at time t such that $\exp[\lambda^{(N_P+1)}t] \ll 1$ we shall also have $\exp[\lambda^{(k)}t] \ll 1$ for values of $k \leq K_T \leq N_P$. However, the above analysis shows that it is not possible to construct a CR model with only K_T states in the P space, because then we would not have $\delta \ll 1$. Thus, in order to construct the correct effective rates, we may have to include in the P space, states which vary more rapidly than than are of direct interest to us.

3. These observation notwithstanding, it may be possible to isolate more than one P space which satisfies the CR model criteria. That is, it may be possible to construct more than one CR model from the same full matrix M.

I conclude with two remarks. First, I have put considerable effort into evaluating the accuracy of the CR model, and have shown that the eigenvalues of the rate matrix M are crucial. They are therefore written out as follows.

stream 93 $i, j, v_i^{(j)}, w_i^{(j)}$, where $v_i^{(j)}$ is the real part, and $w_i^{(j)}$ the imaginary part of the i'th componenent of the eigenvector of the *permuted*[7] matrix M, associated with the j'th eigenvalue of M, where the eigenvalues are arranged in order of increasing absolute value.

stream 94 is identical to stream 93, except that the eigenvectors are those of the *unpermuted ie* the states are in their *original* order *cf* stream 49.

Indeed, the validity of a specific choice of P and Q spaces to construct a CR model, and its properties are uniquely determined by the rate matrix M. Although the program `crmol` is designed to construct the rate matrix for a particular set of processes, it can also be used to analyse any putative rate matrix and and choice of P and Q spaces. In order to do this, we set

```
ifrng = N_P
  nev = eigenvalue selection (see section 3)
```

on `stdin`. All other input on `stdin` is ignored if `ifrng` is positive. The rate matrix must be input on stream 10 in the form

stream 10 $i, j, M(i, j)$

ordered so that the first N_P rows correspond to the P space. Output giving details of the CR model and population coefficients derived from this

[7] *ie* the states are in their *final* order *cf* stream 12.

rate matrix, (but not of course relating to the construction of the rate matrix itself) is produced, as detailed in section 3. Specifically streams 12 (a repetition of stream 10), 21, 22, 87, 91 and 93[8] are then produced.

Finally, if criterion C above is satisfied, then all the Q space states reach equilibrium on a much shorter timescale than the characteristic timescale for the development of the P space states, and, as I have said above, the population coefficients are adequately given by $-\mathbf{M}_Q^{-1}\mathbf{V}$, and $-\mathbf{H}\mathbf{M}_Q^{-1}$. However, these expressions have a simple and illuminating physical interpretation. Suppose $\mathbf{S}_Q^{\text{in}}$ is a given source of Q space densities. Then the equilibrium distribution (i e the distribution of Q space densities for $t \rightarrow \infty$) is given by

$$\mathbf{n}_Q(t \rightarrow \infty) = -\mathbf{M}_Q^{-1}\mathbf{S}_Q^{\text{in}} \tag{84}$$

It is clear from equation 14 that $\mathbf{V}\mathbf{n}_P$ is a source of Q space densities obtained by direct excitation from the P space. Thus, the population coefficient $-\mathbf{M}_Q^{-1}\mathbf{V}$ can be interpreted as a direct excitation from the P space, followed by a rapid equilibration in the Q space. Now

$$\left[-\mathbf{M}_Q^{-1}\mathbf{V}\right]_{fi} = \sum_k \left[-\mathbf{M}_Q^{-1}\right]_{fk} [\mathbf{V}]_{ki} \tag{85}$$

so we may interpret this population coefficient as implying that the final Q space state labelled f in 85 is reached from an initial P space state i through the intermediate states k. In an exactly similar way the expansion

$$\left[-\mathbf{H}\mathbf{M}_Q^{-1}\right]_{fi} = \sum_k [\mathbf{H}]_{fk} \left[-\mathbf{M}_Q^{-1}\right]_{ki} \tag{86}$$

has the interpretaion that the P space state f gets a contribution from the Q space source i through intermediate states k. It is because these decompositions are sometimes useful that $\mathbf{V}$, $\mathbf{H}$ and $\mathbf{M}_Q^{-1}$ are written out separately on streams 80 and 81.

6 Example

I close with an example. This is designed to help with understanding how the code should be used, rather than to explore a physical phenomenon, so only few details of the physics are given. D Wünderlich (2000) has used a CR model very similar (and in part identical) to `crmol` to explore several interesting phenomena, and more details of the relevant physics can be found there.

Consider the important quantity X, the number of Fulcher photons per ground state molecule loss. This can be calculated as

$$X = \frac{2}{9} A_{\text{Fulcher}} n_3^T / \mathcal{R}^{\text{eff}} n_e n_{\text{gs}} \tag{87}$$

[8]The states as specified on stream 10 are deemed to be 'reordered'.

where A_{Fulcher} is the Fulcher Einstein coefficient, n_3^T is the population of the $n = 3$ triplet molecular state, $\mathcal{R}^{\text{eff}}$ is the effective rate coefficient for irretrievable loss of molecules, n_e is the electron density and n_{gs} is the molecular ground state density. The factor 2/9 is the statistical weight of the Fulcher band initial state in the $n = 3$ triplet molecular state. In order to perform this calculation, the following steps must be taken:

1. Construct the input to the CR model (`stdin` and `fort.7`),
2. Run the code and:
   (a) Check for validity,
   (b) Extract the appropriate quantities from the output,
   (c) Form X.

This is the `stdin` input file. Comparison with the format given in section 3 shows that this calculation is performed for $T_e = 20$ eV, $n_e = 10^{13}$ cm^{-3}, with fixed H^+ density (species 65) at the same value, and with 17 states in the P space.

```
-1 1
15 3 20 3 20 20
20 1e13 6 7 8 9 11 37 38
2
1 1
1 65  1e13
1 1
1
17 1
```

The P space states are specified by input on `fort.7`, as follows

```
1 2 3 4  5 6 7 8 9 10 11 12 13 14 15 62 64
```

(all 15 H_2 vibrational levels, H_2^+ and H($1s$))

The most important output is on `fort.21`; part of this output is

```
 GS v=  0   1
 GS v=  1   2
      .
      .
      .
```

```
H(n)= 18  82
H(n)= 19  83
esing 1 is Bsigma
esing 2 is EFsigma
esing 3 is Cpi
etrip 1 is bsigma
etrip 2 is asigma
etrip 3 is cpi
NB in fort.98 and fort.99 the electronically excited states
of the molecule are labelled 1,2 ...N_max=n_explicit+n_rydberg+1
2,3,4 are the explicit states above (S=singlet, T=triplet)
5 .... N_max are the singlet (S) or triplet (T) Rydberg states
and state 1 (S or T) is always the electronic ground state,
which is given honourary triplet status for the purpose of
electronic collisions and radiative recombination
N/A means not applicable - rates so labelled are not used
density fixed for H+        65

The re-ordered matrix labels
final state          1 is GS v=  0   1
final state          2 is GS v=  1   2
final state          3 is GS v=  2   3
     .
     .
     .
final state         16 is H2+    1  62
final state         17 is H(1s)     64
      .
      .
      .
final state         39 is etrip  1  39
final state         40 is etrip  2  40
final state         41 is etrip  3  41
final state         42 is rtrip  1  42
final state         43 is rtrip  2  43
     .
     .
     .

final state         82 is H(n)= 19  83
```

followed by details of the eigenvalues, which I do not reproduce in full here. However, the transition between the P and Q space eigenvalues is significant, and is

```
16  -.297993E+07  -.297994E+07  -.317508E-13   .000000E+00   .772461E-04
17  -.330913E+07  -.330913E+07   .998787E+00   .100000E+01   .127628E-04
 ------------------------------------------------------------------------
18  -.102812E+08  -.102812E+08  -.522986E-17   .000000E+00   .132245E-01
19  -.192484E+08  -.192480E+08  -.577270E-17   .000000E+00   .313804E-01
```

The jump in eigenvalue is reasonably large, and suggests that the population coefficients are adequately given by $-\mathbf{M}_Q^{-1}\mathbf{V}$. This is confirmed by examining stream 87, which also shows that the CR model satisfies the accuracy criterion described above.

The relevant part of `fort.87` is

```
 1      .1213E-02     .2926E-02     .1400E-01     .1800E-02
 2      .1120E-02     .2946E-02     .1430E-01     .1826E-02
 3      .6081E-03     .1608E-02     .1481E-01     .1867E-02
 4      .6647E-03     .1763E-02     .2669E-01     .1892E-02
 5      .6948E-03     .1857E-02     .2578E-01     .1952E-02
 6      .3071E-03     .8040E-03     .2818E-01     .2038E-02
 7      .2073E-03     .5566E-03     .3437E-01     .2181E-02
 8      .9428E-04     .2400E-03     .3159E-01     .2163E-02
 9      .1010E-03     .2647E-03     .2726E-01     .2128E-02
10      .1864E-03     .4926E-03     .2830E-01     .2154E-02
11      .6569E-04     .1570E-03     .2643E-01     .2148E-02
12      .5389E-04     .1348E-03     .2671E-01     .2150E-02
13      .5360E-04     .1352E-03     .2689E-01     .2134E-02
14      .4933E-04     .1246E-03     .2710E-01     .2088E-02
15      .3982E-04     .1014E-03     .2740E-01     .2014E-02
16      .2174E-04     .5550E-04     .1771E-02     .1124E-02
17      .3612E-05     .9150E-05     .1487E-02     .1212E-02
```

showing that the calculation is indeed valid.

Now, according to the output, the initial state for the Fulcher transition — `rtrip 1` — is state 42. Since there are 17 P space states it is state 25 (= 42-17) in the Q space. The $H_2(v = 0)$ state has index 1, and therefore also index 1 in the P space. Thus, the required population coefficient is in `fort.33` ($\mathbf{M}_Q^{-1}\mathbf{V}$), or `fort.34` ($\delta\mathbf{T}_P^{-1}$), in each case, with index $\{25, 1\}$. The values are

```
fort.33  8.0970E-005
fort.34  8.2346E-005
```

As expected, they are close. The value of $\mathcal{R}^{\text{eff}} n_e$ can be obtained from `fort.22`. According to `fort.21` above, states 1 to 15 represent all the H_2 states. Thus, from equation 19 we see that the total rate of molecular loss

is, in general, given by[9]

$$\mathcal{R}^{\text{eff}} n_e = -\sum_{k=1}^{15} \dot{n}_k = \sum_{k=1}^{N_P} \left\{ -\sum_{j=1}^{15} [\mathrm{M}_{\text{eff}}]_{j,k} \right\} n_k \tag{88}$$

so that, since we are assuming that only the ground vibrational state ($k = 1$) is occupied, we have

$$\mathcal{R}^{\text{eff}} n_e = \left\{ -\sum_{j=1}^{15} [\mathrm{M}_{\text{eff}}]_{j,1} \right\} n_1 \tag{89}$$

Performing this sum we get $\mathcal{R}^{\text{eff}} n_e$ =367896.24

Finally, the A_{Fulcher} can be obtained from `fort.99`, where line 1491 reads

```
2.000000000000000E+007  1491          .200000E+08 T   3 <- rad   5
```

This is labelled as corresponding to the radiative transition (`rad`) from triplet state (T) 5 (`rtrip 1`) to 3 `etrip 2`, *i e* $^3a\Sigma$). A reminder of how the states are labelled is helpfully written on stream 21.

Putting this all together gives (using the more accurate `fort.34`) result

$$X = 9.95 \times 10^{-4} \text{ photons/mol}$$

Similar calculations performed at different temperatures and densities lead to results for the number of Fulcher photons/ground state molecule loss such as

n_e cm^{-3}	$T_e = 5$ eV ($N_P = 18$)	$T_e = 20$ ($N_P = 17$)
10^8	2.04×10^{-3}	8.21×10^{-4}
10^{10}	3.88×10^{-3}	1.89×10^{-3}
10^{11}	3.82×10^{-3}	1.88×10^{-3}
10^{12}	3.37×10^{-3}	1.65×10^{-3}
10^{13}	2.25×10^{-3}	9.95×10^{-4}
10^{14}	6.00×10^{-4}	2.39×10^{-4}
10^{15}	6.08×10^{-5}	2.60×10^{-5}

The number of Fulcher photons/ground state molecule loss through dissociation, ionization and, for $T = 5$ eV, H^- production.

[9] In this case there is no contribution from Γ'_P.

Finally I should remark that not all aspects of this code have been fully tested, and it is still undergoing development. Further information will be provided as it becomes available.

The program `crmol` is based in part on an original code developed by T Fujimoto and K Sawada, and I would like to thank them for making the code available. I have enjoyed useful discussions with D Reiter of Düsseldorf, U Fantz and D Wünderlich of Augsburg, A Pospieszczyk S Brezinsek and G Servienko of FZ-Jülich. This work was done under Contract no 414-014-02 with FZ-Jülich, D-52425 Jülich, Germany.

7 Appendix 1 The Janev Rates

The input for molecular processes in the ground electronic state.

`nproc ipick(3+k),k=1,nproc`. This sets the molecular collision processes. `nproc` is the number of processes, and `k` their index. The code automatically sets `ipick(1)` =1 and `ipick(2)` =2 to include $\Delta v = 1$ and $\Delta v = 2$ electron-molecule vibrational excitation, and `ipick(3)` =10 to include impact ionization of H_2. It is assumed that this rate is independent of the vibrational level of the H_2. The other processes are identified below in the following table 'The Janev rates' (Janev, 1987). These processes are not resolved with respect to the vibrational level of the ground state in Janev et al., 1987, but, instead, are rates for the processes starting from the vibrational ground state of the electronic ground state of the molecule.

For this reason we presently use scaling laws. The processes marked † in the table have such scaling laws. We have based these laws on data for cross sections of vibrationally excited states. The actual laws used are listed below.

Furthermore:

Reaction 37 is identical to reaction 13 (Ion Conversion) for molecular excitation up to $v = 3$, but has a rate equal to resonant charge transfer ($H(1s) + p \rightarrow p + H(1s)$) for all higher vibrational states. It thus represents a different scaling law for IC to what is described in Greenland & Reiter (1996). The inverse reaction rate is unchanged. As a result Dissociative Attachment (DA), (which is not taken from Janev, 1987) now has index number **38.**

The Janev rates

The code is supposed to make a compromise between simplicity and flexibility, so that most of the rates are calculated by default. Only the selection of some molecular processes is under the user's control. The present situation

is as follows:

1. Processes 11 (ionization + dissociation), 13/37 (IC) and 38 (DA) are the only valid choices. Processes 6 (Diss) and 10 (molecular ionization) will be included correctly, but will lead to double counting, and should therefore NOT be included if the results are to correspond to physical reality.

2. The recombination processes 25 to 28 are automatically added to the coupling matrix.

3. If, and only if process 38 is specified, then H^- is produced, and processes 19, 20 and 21, as well as processes 29 and 30 are potentially included. Note however, that processes 19, 20 and 21 involve $H^- - p$ collisions, and are therefore only included in fact, if either the proton or H^- density is specified to be fixed.

4. The ion conversion process 13 or 37 is only allowed in the forward direction if either the proton or H_2 density is fixed, and in the backward direction if either the H or H_2^+ density is fixed. If the appropriate condition is not met, the rate for the Ion Conversion process (or its inverse) is automatically set to zero, even if process 13 or 37 is selected.

The following rates from Janev, 1987 are available in an internal database in the code (function epick):

There is a complication for heavy particle collisions. Janev *et al* tabulate rates for fixed heavy projectiles with fixed velocity traversing a target of given temperature, whereas we require the rates for the circumstance in which both projectile and target have effective temperatures. However it is not difficult to show that

$$S_2(T_1, T_2) = S_1(T_{\text{eff}}) = < \sigma v >_{V \to 0} (T_{\text{eff}}) \qquad (1a)$$

where $S_2(T_1, T_2)$ is the rate coefficient for collisions between particles of type 1 at temperature T_1 and particles of type 2 at temperature T_2, $S_1(T_{\text{eff}})$ is the rate coefficient for stationary particles of type 2 in a bath of particles of type 1 at temperature T_{eff}, and $< \sigma v >_V (T)$ is the quantity tabulated by Janev *et al*, that is the rate coefficient for collisions between particles of type 1 at temperature T in collision with a beam of particles of type 2 with velocity V. We have

$$T_{\text{eff}} = \frac{M}{M_1} T_1 + \frac{M}{M_2} T_2 \qquad (1b)$$

where M_1 and M_2 are the masses of particles of types 1 and 2 respectivly, and M is the mass of the target particles[10] used in preparing the tables of

[10] *ie* those particles whose velocities are assumed to be thermally distributed in the tabulation of $< \sigma v >_V (T)$, that is, particles of type 1 as described here

$< \sigma v >_V (T)$. In the table below the 'particle of type 1' is always listed *first* in the description of the reaction, so that t_r, the correction factor, defined so that the correct rate coefficient to use for the reaction is

$$S =< \sigma v >_{V \to 0} [(1 + t_r)T] \tag{2}$$

is given by M_1/M_2. In equation 2 T is the plasma temperature; I assume that the heavy particles have the same temperature. (If the heavy particles are assumed to be stationary, as is always effectively the case with heavy particles in an electron bath at temperature T, then $t_r = 0$.) Notice that *except for rate 18* we always have $t_r \leq 1$. In fact, the smallest valid value of V given by Janev *et al*'s fitting expression corresponds to a heavy particle energy of E = 0.1 eV. At present, our tabulation uses a value of E = 0.37 eV (log(E)=-1.).

The scaling laws for vibrational state resolved rates

The processes marked † have scaling laws based on data for cross sections of vibrationally excited states. The actual laws used are

For process 1

$$S_{k(>v)\leftarrow v} = \frac{e^{[5E_v - 4.44E_k]}}{0.121} S_{1\leftarrow 0} \tag{3}$$

based on a fit to cross section data from Bardsley and Wadehra (1979). The rate $S_{k(<v)\leftarrow v}$ is obtained by detailed balance.

For process 6

$$S_v = \frac{e^{-0.07E_v}}{1.0019} S_0 \tag{4}$$

based on cross section data from Rescignio and Schneider (1988). *These rates are superceded by direct excitation to the* $^3b\Sigma$ *state, for which some vibrationally resolved data is available. This is discussed in Appendix 3.*

For process 10

$$S_v = S_0 \tag{5}$$

For process 13

$$S_v = \frac{3.36 S_0}{0.0202 + (2.1 - E_v)^2} \tag{6}$$

based on a Lorenzian designed to give a total capture cross section equal to the $H - H^+$ resonant charge transfer cross section at zero energy defect.

In the above formulae, E_v is the *excitation* energy, in eV of the state with vibrational quantum number v (including the zero point energy), given by

$$E_v = 0.545666(v + \frac{1}{2}) - 0.015044(v + \frac{1}{2})^2 \tag{7}$$

and S_0 ($S_{1\leftarrow 0}$) is the rate for the process in the ground vibrational state given by Janev *et al.* S_v ($S_{k(>v)\leftarrow v}$) is the rate for the corresponding process starting in the vibrational level v.

Dissociative Attachment

The rate coefficients for processes

$$e + \mathrm{H_2(v)} \rightarrow \mathrm{H^-} + \mathrm{H}$$

have been fitted to a simple analytic form, based on a fit to the cross sections of Bardsley and Wadehra (1979): *viz*

$$S_v(T) \sim 6.69 \times 10^7 \sigma_v^{\mathrm{thresh}} \sqrt{T} \frac{1 + (\alpha T + 1)\frac{E_v}{T}}{(1 + \alpha T)^2} \exp\{-E_v/T\} \qquad (8)$$

where $S_v(T)$ is the rate coefficient ($\mathrm{cm^3\,s^{-1}}$ at temperature T (eV), E_v is the *threshold* energy (in eV) for dissociative attachment from the v'th vibrational level, and $\sigma_v^{\mathrm{thresh}}$ is the corresponding threshold cross section (in $\mathrm{cm^2}$). The parameter α has the mean value

$$\alpha \sim 2.27 \ \ (\mathrm{eV})^{-1}$$

In fact, each vibrational level has its own value of α, and these, together with the threshold cross sections and energies are shown below.

State v	1	2	3	4	5
σ_{thresh}	2.5^{-21}	1.3^{-19}	1.3^{-18}	8.9^{-18}	5^{-17}
α	1.66	2.37	2.06	2.36	2.35
E_v	3.763	3.237	2.763	2.316	1.868
State v	6	7	8	9	10
σ_{thresh}	1.6^{-16}	4.5^{-16}	4^{-16}	3.2^{-16}	4.5^{-16}
α	2.29	2.32	2.21	2.27	2.15
E_v	1.474	1.079	0.737	0.421	0.132

Table 1: The threshold cross sections $\mathrm{cm^2}$ and energies (eV) for the first 10 states in $\mathrm{H_2}$, and the values of α ($\mathrm{eV^{-1}}$) a^b means $a \times 10^b$.

Expression 1 agrees with what was given by Wadehra at the IAEA meeting on molecular processes, and the DA rates calculated with it and the values tabulated above agree with results by Biel of Düsseldorf (PHD Thesis).

Finally I gve expressions for the electron energy loss derived from equation 18h. Three cases are important:

Radiative recombination: Sawada and Fujimoto (1995) use

$$\alpha_p(T) \propto \left(\frac{E_p}{T}\right)^{3/2} \int_0^{20T/E_p} du$$

$$\left[\frac{1}{1+u} + \frac{0.1728(u-1)}{p^{3/2}(u+1)^{5/2}} - \frac{0.0496(u^2+4u/3+1)}{p^{4/3}(u+1)^{7/3}}\right] \exp(-uE_p/T) \tag{9a}$$

for the radiative recombination rate coefficient into the state with principal quantum number p and binding energy E_p. This gives

$$\mathcal{S}_p(T) \propto \left(\frac{E_p}{T}\right)^{3/2} E_p \int_0^{20T/E_p} u\, du$$

$$\left[\frac{1}{1+u} + \frac{0.1728(u-1)}{p^{3/2}(u+1)^{5/2}} - \frac{0.0496(u^2+4u/3+1)}{p^{4/3}(u+1)^{7/3}}\right] \exp(-uE_p/T) \tag{9b}$$

for the corresponding energy loss rate coefficient.

Equation 8 gives

$$\mathcal{S}_v^{\mathrm{DA}} = S_v(T)\left[\frac{2T}{1+\alpha T} + \frac{E_v^2(1+\alpha T)}{T+E_v(1+\alpha T)}\right] \tag{10}$$

where $S_v(T)$ is given in equation 8 and the parameters α and E_v are given in Table 1.

For the polynomial fit to the rates used extensivly here, we have

$$\frac{\partial \mathcal{R}(\beta)}{\partial \beta} = T\sum_1^8 n b_n \left[\ln(T)\right]^{(n-1)} \tag{11}$$

wherce $\mathcal{S}$ may be obtained.

The Janev rates are shown below. The subroutine which calculates the rates will calculate all those listed, but at present only rates number 1, 2, 3, 4, 5, 6, 7, 8, 9, 10, 11, 13/37, 19, 20, 21, 25, 26, 27, 28, 29, and 30 are included in `crmol`. Better rates than those given by Janev are used for processes 3, 4, 5, and 6. (see appendicies 2 and 3 for more details).

Index	Section	$M_1 + M_2 \rightarrow$ products	process	t_r
$\rightarrow$ †1	2.2.1a	$e+H_2(v=0) \rightarrow e+H_2(v=1)$	vib excitation $\Delta v = 1$	0
$\rightarrow$ 2	2.2.1b	$e+H_2(v=0) \rightarrow e+H_2(v=2)$	vib excitation $\Delta v = 2$	0
3	2.2.2	$e+H_2 \rightarrow e+H_2^*$	electronic excitation	0
4	2.2.3	$e+H_2 \rightarrow e+H_2^*$	electronic excitation	0
5	2.2.4	$e+H_2 \rightarrow e+H_2^*$	electronic excitation	0
$\rightarrow$ †6	2.2.5	$e+H_2 \rightarrow e+H+H$	impact dissociation (Diss)	0
7	2.2.6	$e+H_2 \rightarrow e+H+H^*$	impact dissociation	0
8	2.2.7	$e+H_2 \rightarrow e+H^*+H^*$	impact dissociation	0
9	2.2.8	$e+H_2 \rightarrow e+H+H^*$	impact dissociation	0
$\rightarrow$ 10	2.2.9	$e+H_2 \rightarrow e+H_2^+ +e$	ionization	0
11	2.2.10	$e+H_2 \rightarrow e+H^+ +H+e$	ionization+dissociation	0
12	3.2.2	$p+H_2(v=0) \rightarrow p+H_2(v>0)$	proton vibrational excitation	0.5
$\rightarrow$ †13	3.2.3	$p+H_2 \rightarrow H(1s)+H_2^+$	ion conversion (IC)	0.5
14	3.2.4a	$p+D_2 \rightarrow D^+ +HD$ (or H+D)	p–d exchange	0.25
15	3.2.4b	$p+D_2 \rightarrow D+HD^+$	p–d exchange	0.25
16	3.2.5	$p+H_2 \rightarrow p+H_2^+(v \leq 9)+e$	proton impact ionization	0.5
17	3.2.6	$p+H_2^+ \rightarrow p+H(1s)+H^+$	proton impact dissociation	0.5
18	4.2.1	$H_2^+ +H(1s) \rightarrow H^+ +H+H(1s)$	hydrogen impact dissociation	2.0
19	7.2.1	$p+H^- \rightarrow p+H+e$	proton impact detachment	1.0
$\rightarrow$ 20	7.2.2	$p+H^- \rightarrow H^*(n=2)+H(1s)$	mutual neutralization (MN)	1.0
$\rightarrow$ 21	7.2.3	$p+H^- \rightarrow H^*(n=3)+H(1s)$	mutual neutralization	1.0
22	7.3.1	$H^- + H(1s) \rightarrow H(1s)+H^-$	charge exchange	1.0
23	7.3.2a	$H^- +H \rightarrow H+H+e$	hydrogen impact detachment	1.0
24	7.3.2b	$H^- +H \rightarrow H_2+e$	associative detachment	1.0
25	2.2.11	$e+H_2^+ \rightarrow e+H^+ +H^+ +e$	breakup	0
$\rightarrow$ 26	2.2.12	$e+H_2^+ \rightarrow e+H^+ +H(1s)$	dissociation	0
$\rightarrow$ 27	2.2.13	$e+H_2^+ \rightarrow e+H^+ +H^*(n=2)$	dissociation	0
$\rightarrow$ 28	2.2.14	$e+H_2^+ \rightarrow H(1s)+H^*(n)$	dissociative recombination (DR)	0
$\rightarrow$ 29	7.1.1	$e+H^- \rightarrow e+H(1s)+e$	electron impact detachment (Det)	0
30	7.1.2	$e+H^- \rightarrow e+H^+ +2e$	detachment and ionization	0
31	2.1.8	$e+H^+ \rightarrow H^*(n) + h\nu$	radiative recombination	0
$\rightarrow$ 32	2.2.15(a/b)	$e+H_3^+ \rightarrow 3H/H_2+H^*$	H_3^+ neutralization	0
$\rightarrow$ 33	2.2.16	$e+H_3^+ \rightarrow e+H^+ + 2H$	H_3^+ breakup	0
$\rightarrow$ 34	4.3.3	$H_2^+ + H_2 \rightarrow H_3^+ + H$	H_3^+ production	1.0
$\rightarrow$ 35	7.3.2a	$H^- + H \rightarrow H+H+e$	H impact dissociation	1.0
$\rightarrow$ 36	7.3.2a	$H^- + H \rightarrow H_2 + e$	associative detachment	1.0
$\rightarrow$ †37	3.2.3	$p+H_2 \rightarrow H(1s)+H_2^+$	ion conversion (IC)	0.5

8 Appendix 2 Vibrationally Resolved Decays

Celiberto & Janev (1995) give fits for the vibrationally resolved cross sections for electron impact excitation of two electronic states in H_2 and D_2.

$$H_2(X^1\Sigma_g)(v) + e \rightarrow H_2(B^1\Sigma_u)$$

and

$$H_2(X^1\Sigma_g)(v) + e \rightarrow H_2(C^1\Pi_u)$$

Each of these excited states supports a vibrational manifold, and the Einstein A coefficients for the radiative decays

$$H_2(B^1\Sigma_u)(v) \rightarrow H_2(X^1\Sigma_g)(v_f) + h\nu$$

and

$$H_2(C^1\Pi_u)(v) \rightarrow H_2(X^1\Sigma_g)(v_f) + h\nu$$

have been tabulated by Allison & Dalgarno (1970). By assuming that electron impact excitation of the upper electronic level leads to a specific distribution of vibrational states in the excited manifold it is possible to calculate the mean radiative decay rate for electronically excited $H_2(B^1\Sigma_u)$ and $H_2(C^1\Pi_u)$. We assume that if the electronic state is excited from an initial vibrational state v_0, then each member of the upper vibrational manifold v is occupied with a probability proportional to the square of the dipole matrix element for the $v \rightarrow v_0$ transition[11]. This leads to a distribution in the excited manifold that depends upon v_0, the vibrational state from which the excitation took place. We remove this dependence by simply averaging over v_0. This now gives a distribution of excited vibrational states independent of the excitation mechanism. The final A value for decay to v_f, a vibrational state of the electronic ground state, is then given by averaging the A values for decay to v_f over this distribution. That is, we calculate the probability of exciting v from v_0 as

$$p_{v,v_0} = \mathcal{D}^2_{v,v_0}/\mathcal{N}_{v_0} \tag{1}$$

where $\mathcal{D}_{v,v_0}$ is the dipole matrix element for the $v_0 \leftarrow v$ transition and

$$\mathcal{N}_{v_0} = \sum_v \mathcal{D}^2_{v,v_0} \tag{2}$$

We now assume that $P(v)$, the 'average' distribution of v can be got from by averaging p_{v,v_0} over the initial vibrational states $0, 1, \cdots v_0, \cdots N$

$$P(v) = \frac{1}{N+1} \sum_{v_0=0}^{N} p_{v,v_0} \tag{3}$$

[11]This can be obtained from the A value and energy difference between the two states.

Finally $\bar{A}_{v_f}$, the mean decay rate from the electronically excited state to the vibrational state v_f in the ground electronic state is given by

$$\bar{A}_{v_f} = \sum_{v}^{N^*} A_{v_f,v} P(v) \tag{4}$$

where the sum runs over the vibrational manifold supported by the excited electronic state, and $A_{v_f,v}$ is the Einstein A coefficient for the $v_f \leftarrow v$ radiative decay. Radiative decay from each of these states to the $X^1\Sigma$ vibrational continuum (which therefore leads to dissociation) is also possible, and its A value can be calculated similarly.

The values used are tabulated below. Clearly other strategies are possible, and the sensitivity of the results to this averaging should be explored. The data are available.

v	$B^1\Sigma$	$C^1\Pi$
0	8.2772736×10^7	1.0298930×10^8
1	7.5957320×10^7	8.5425808×10^7
2	6.8873384×10^7	6.4538444×10^7
3	6.7167080×10^7	6.0403508×10^7
4	6.3768032×10^7	6.3656576×10^7
5	6.3601840×10^7	6.0684180×10^7
6	5.9270400×10^7	5.9209288×10^7
7	5.7115708×10^7	6.1643808×10^7
8	5.3714124×10^7	6.1465744×10^7
9	5.1850780×10^7	6.2449096×10^7
10	4.8581508×10^7	6.5405168×10^7
11	4.6469164×10^7	6.7786120×10^7
12	4.4187192×10^7	6.9719520×10^7
13	3.8139332×10^7	6.8034384×10^7
14	2.2083192×10^7	4.8494500×10^7
∞	2.8110592×10^8	1.0094800×10^8

Table 1: The effective A values (s^{-1}) for decay from the $B^1\Sigma$ and $C^1\Pi$ states to the vibrational levels of the ground state. Also shown, as $v = \infty$ are the radiative decay rates to the vibrational continuum of the ground state.

9 Appendix 3 The $n = 2$ Rates

New cross section data for excitation of the $n = 2$ singlet states $B^1\Sigma$, $C^1\Pi$ and the triplet state $b^3\Sigma$ from the vibrational levels of the $X^1\Sigma$ ground state are available. Rates based on these new data are incorporated into the code. They are described here.

The singlet state rates are straightforward. Celiberto and Janev (1995) give expressions for the electron impact excitation cross section for the processes

$$\mathrm{H}_2[X^1\Sigma](v) + \mathrm{e} \rightarrow \sum_{v'} \mathrm{H}_2[B^1\Sigma](v') + \mathrm{e} \qquad (1a)$$

and

$$\mathrm{H}_2[X^1\Sigma](v) + \mathrm{e} \rightarrow \sum_{v'} \mathrm{H}_2[C^1\Pi](v') + \mathrm{e} \qquad (1b)$$

and these can be converted to rates by integrating over a Maxwell-Boltzmann distribution of velocities for a given temperature T. We have, for the rate $\mathcal{R}$,

$$\mathcal{R}(T) = \frac{4}{\sqrt{\pi}} \left(\frac{kT}{2m}\right)^{1/2} \int dx \; x\sigma(x\,kT) \exp(-x) \qquad (2)$$

where m is the electron mass, $\sigma(E)$ the cross section at electron impact energy E and kT the energy associated with temperature T. Usually T is measured in eV, so that k is suppressed. These rates can be fitted as (Janev *et al* 1987)

$$\ln(\mathcal{R}(T)) = \sum_{k=0}^{8} b_k (\ln(T))^k \tag{3}$$

The coefficients b_k are given in table 1, and the fits are compared with the 'true' rates, derived directly from equation 2 in figures 1 and 2. These fits, and therefore the code itself cease to be reliable below an electron temperature of 0.5 eV.

Table 1: The coefficients for the $B^1\Sigma$ excitation from the ground state vibrational levels (equation 3) in the order

b_0 b_1 b_2
b_3 b_4 b_5
b_6 b_7 b_8

Vib. level no.	1	B state
-0.2880946E+02	0.9541977E+01	-0.3966258E+01
0.1080775E+01	-0.2065085E+00	0.2690762E-01
-0.2253846E-02	0.1086306E-03	-0.2279712E-05
Vib. level no.	2	B state
-0.2816380E+02	0.9400263E+01	-0.4170421E+01
0.1253500E+01	-0.2667564E+00	0.3837598E-01
-0.3494823E-02	0.1803441E-03	-0.3999552E-05
Vib. level no.	3	B state
-0.2646792E+02	0.1037208E+02	-0.6565566E+01
0.2694575E+01	-0.7057833E+00	0.1153278E+00
-0.1135514E-01	0.6156517E-03	-0.1410782E-04
Vib. level no.	4	B state
-0.2700517E+02	0.8874048E+01	-0.4168608E+01
0.1355566E+01	-0.3117252E+00	0.4779701E-01
-0.4572125E-02	0.2449583E-03	-0.5592066E-05
Vib. level no.	5	B state
-0.2689817E+02	0.9289897E+01	-0.4689720E+01
0.1663134E+01	-0.4132763E+00	0.6734438E-01
-0.6745774E-02	0.3743037E-03	-0.8779752E-05
Vib. level no.	6	B state
-0.2599713E+02	0.8826899E+01	-0.4892533E+01
0.1934503E+01	-0.5211576E+00	0.8940473E-01
-0.9249642E-02	0.5241729E-03	-0.1247418E-04
Vib. level no.	7	B state
-0.2584816E+02	0.8795786E+01	-0.4832247E+01
0.1885146E+01	-0.5028363E+00	0.8574919E-01
-0.8841014E-02	0.5000067E-03	-0.1188453E-04

$B^1\Sigma$ *continued*

Vib. level no.	8	B state
-0.2570931E+02	0.8763256E+01	-0.4780183E+01
0.1843632E+01	-0.4873893E+00	0.8264650E-01
-0.8491882E-02	0.4792400E-03	-0.1137539E-04
Vib. level no.	9	B state
-0.2562608E+02	0.8767379E+01	-0.4755383E+01
0.1816035E+01	-0.4762224E+00	0.8032676E-01
-0.8226280E-02	0.4632726E-03	-0.1098098E-04
Vib. level no.	10	B state
-0.2554579E+02	0.8742564E+01	-0.4722188E+01
0.1790030E+01	-0.4665302E+00	0.7837564E-01
-0.8006431E-02	0.4501871E-03	-0.1066007E-04
Vib. level no.	11	B state
-0.2470037E+02	0.7878417E+01	-0.4423302E+01
0.1787829E+01	-0.4930125E+00	0.8625272E-01
-0.9064225E-02	0.5201051E-03	-0.1250256E-04
Vib. level no.	12	B state
-0.2467941E+02	0.7636692E+01	-0.4073292E+01
0.1562898E+01	-0.4164065E+00	0.7138478E-01
-0.7411070E-02	0.4220068E-03	-0.1009312E-04
Vib. level no.	13	B state
-0.2471478E+02	0.7599960E+01	-0.4091470E+01
0.1588046E+01	-0.4265000E+00	0.7344852E-01
-0.7644017E-02	0.4358356E-03	-0.1043086E-04
Vib. level no.	14	B state
-0.2490949E+02	0.7596427E+01	-0.4140032E+01
0.1632552E+01	-0.4431187E+00	0.7674929E-01
-0.8011485E-02	0.4575168E-03	-0.1095941E-04
Vib. level no.	15	B state
-0.2542487E+02	0.6270535E+01	-0.1908366E+01
0.1817239E+00	0.4856512E-01	-0.1807688E-01
0.2474441E-02	-0.1619281E-03	0.4199320E-05

Table 1: The coefficients for the $C^1\Pi$ excitation from the ground state vibrational levels (equation 3) in the order

b_0 b_1 b_2
b_3 b_4 b_5
b_6 b_7 b_8

Vib. level no.	1	C state
-0.2857195E+02	0.5632497E+01	0.7977110E+00
-0.1490994E+01	0.5577894E+00	-0.1065450E+00
0.1139347E-01	-0.6482104E-03	0.1530057E-04
Vib. level no.	2	C state
-0.2946878E+02	0.1085519E+02	-0.5329912E+01
0.1806569E+01	-0.4228390E+00	0.6486939E-01
-0.6156049E-02	0.3261565E-03	-0.7358407E-05
Vib. level no.	3	C state
-0.2942827E+02	0.1140928E+02	-0.6052835E+01
0.2212955E+01	-0.5472789E+00	0.8712384E-01
-0.8477170E-02	0.4570236E-03	-0.1044118E-04
Vib. level no.	4	C state
-0.2866825E+02	0.1091710E+02	-0.6087700E+01
0.2357643E+01	-0.6103653E+00	0.1004025E+00
-0.1000106E-01	0.5485920E-03	-0.1269968E-04
Vib. level no.	5	C state
-0.2853465E+02	0.1081087E+02	-0.5994744E+01
0.2307427E+01	-0.5949813E+00	0.9765049E-01
-0.9714267E-02	0.5324354E-03	-0.1231922E-04
Vib. level no.	6	C state
-0.2840971E+02	0.1073600E+02	-0.5928291E+01
0.2271533E+01	-0.5841094E+00	0.9573585E-01
-0.9518031E-02	0.5215611E-03	-0.1206717E-04
Vib. level no.	7	C state
-0.2828849E+02	0.1066558E+02	-0.5862852E+01
0.2235988E+01	-0.5732832E+00	0.9381127E-01
-0.9318397E-02	0.5103530E-03	-0.1180397E-04

$C^1\Pi$ *continued*

Vib. level no.	8	C state
-0.2820876E+02	0.1062623E+02	-0.5810473E+01
0.2203819E+01	-0.5630673E+00	0.9196823E-01
-0.9126409E-02	0.4995754E-03	-0.1155132E-04
Vib. level no.	9	C state
-0.2813241E+02	0.1058803E+02	-0.5767167E+01
0.2178312E+01	-0.5550197E+00	0.9050752E-01
-0.8972426E-02	0.4908049E-03	-0.1134253E-04
Vib. level no.	10	C state
-0.2730959E+02	0.1018978E+02	-0.6040713E+01
0.2487793E+01	-0.6740528E+00	0.1144270E+00
-0.1165286E-01	0.6496249E-03	-0.1522529E-04
Vib. level no.	11	C state
-0.2723168E+02	0.1015865E+02	-0.6025519E+01
0.2482513E+01	-0.6729944E+00	0.1143225E+00
-0.1164971E-01	0.6497651E-03	-0.1523332E-04
Vib. level no.	12	C state
-0.2714137E+02	0.1021126E+02	-0.6193227E+01
0.2618537E+01	-0.7255460E+00	0.1253963E+00
-0.1295543E-01	0.7307295E-03	-0.1729075E-04
Vib. level no.	13	C state
-0.2707138E+02	0.1020464E+02	-0.6210808E+01
0.2633121E+01	-0.7307149E+00	0.1264001E+00
-0.1306640E-01	0.7372746E-03	-0.1745068E-04
Vib. level no.	14	C state
-0.2701894E+02	0.1009277E+02	-0.6093401E+01
0.2568586E+01	-0.7101654E+00	0.1225234E+00
-0.1263999E-01	0.7120533E-03	-0.1683134E-04
Vib. level no.	15	C state
-0.2710058E+02	0.1019981E+02	-0.6202807E+01
0.2629292E+01	-0.7287225E+00	0.1258238E+00
-0.1298162E-01	0.7311730E-03	-0.1727901E-04

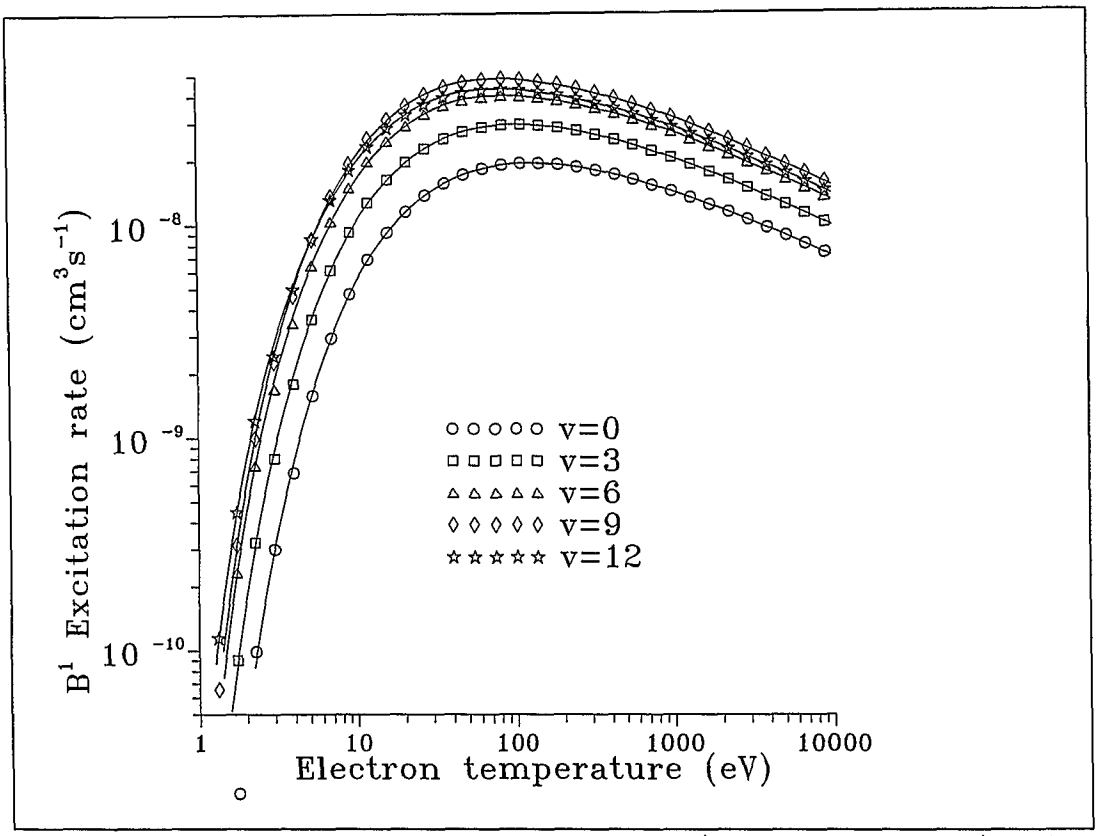

Figure 1: Comparison between the 'true' rates (equation 2, symbols) and the polynomial fits (equation 3, lines) for selected excitation rates to the $B^1\Sigma$ state

The $b^3\Sigma$ state is less straightforward. Two sets of theoretical results for the process

$$H_2[X^1\Sigma](v) + e \rightarrow H_2[b^3\Sigma](v) + e \rightarrow H + H + e \tag{4}$$

are available. The calculations of Rescignio and Schneider (1988) are expected to be more accurate for high energy (> 20 eV) electron impact, whereas more recent calculations of Stibbe and Tennyson (1998) give a good account of the threshold region, but underestimate the cross section for impact energies > 12 eV. These authors stress that the threshold for excitation from vibrationally excited states is *lower* than would be expected if 'vertical' transitions were dominant. The circumstance that the excitation is dominated by the 'outer' Franck-Condon region leads to a greater reduction in threshold with increasing vibrational quantum number than the reduction in energy defect would imply. In order to include both sets of data, a least squares fit of the cross section to the function

$$\sigma_F(E) = A_1 \frac{(E - A_2)^{A_3} \exp(-A_4 E)}{1 + A_5 E + A_6 E^2 + A_7 E^3} \tag{5a}$$

was performed. Points were weighted so that the Stibbe-Tennyson results dominated at low energy, whereas the Rescignio-Schneider cross sections were

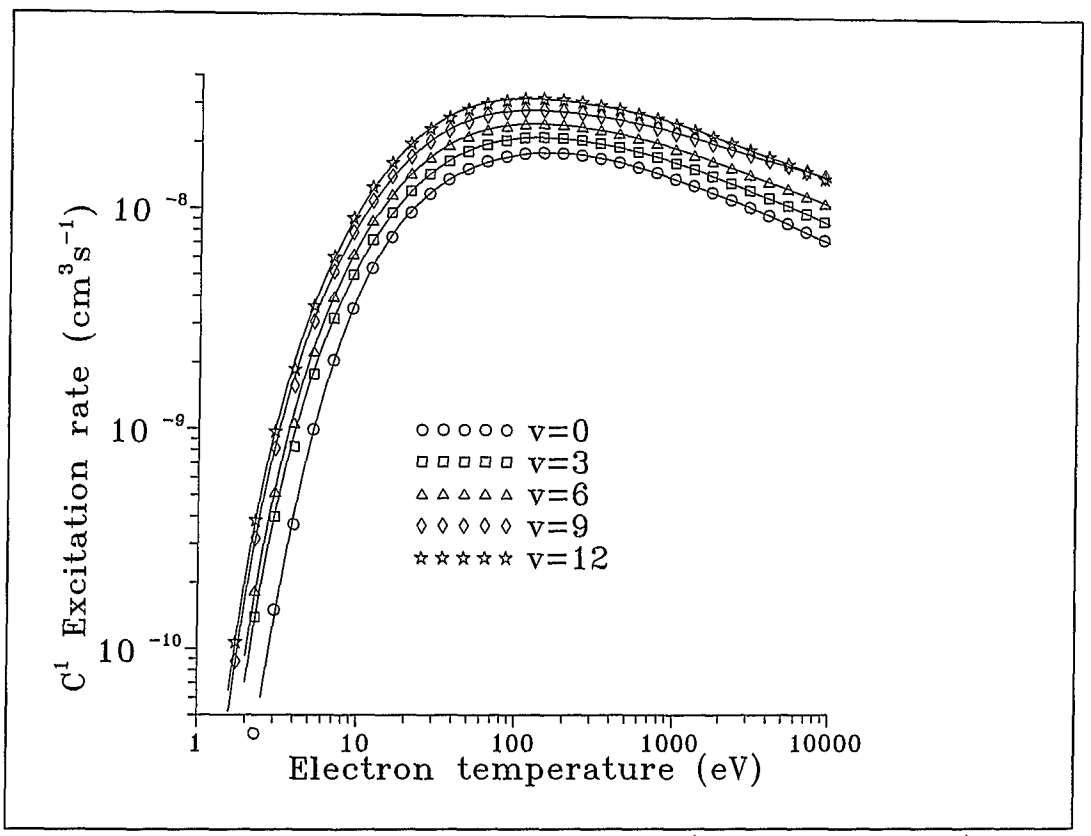

Figure 2: Comparison between the 'true' rates (equation 2, symbols) and the polynomial fits (equation 3, lines) for selected excitation rates to the $C^1\Pi$ state

decisive at high energy. The resulting fitting parameters $A_1 \cdots A_7$, and the corresponding cross sections are shown in table 3 and figure 3 respectivly. For energies higher than 30 eV we assume that the cross section can be adaquatly represented as

$$\sigma(E > 30\,\mathrm{eV}) = B_v \left(\frac{30}{E}\right)^{2.744} \tag{5b}$$

with B_v given in table 4.

	$v=0$	$v=1$	$v=2$
A_1	0.00065788575	0.00001141831	0.00018860681
A_2	5.25773110240	3.68588625448	3.48256259480
A_3	4.59403968684	6.89544476148	5.69787818749
A_4	0.14914035747	0.36832502752	0.31334457034
A_5	0.04788913323	-0.26485979837	-0.31281368492
A_6	-0.02963216007	0.02098684002	0.02873647208
A_7	0.00182956069	-0.00038791382	-0.00055229315
	$v=3$	$v=4$	
A_1	0.00996801496	0.01406128828	
A_2	3.89560057617	3.14160375973	
A_3	3.56358107842	3.47828561773	
A_4	0.14322854653	0.14018118148	
A_5	-0.35265064569	-0.40760456965	
A_6	0.03254051095	0.04426936101	
A_7	-0.00002921044	-0.00017458941	

Table 3: The fits for the cross sections for electron impact excitation of the $b^3\Sigma$ state from the $v = 0 \cdots 4$ vibrational levels of the ground state.

	$v=0$	$v=1$	$v=2$	$v=3$	$v=4$
B_v	0.7507	0.7668	0.7849	0.8099	0.8203

Table 4: The coefficients for the tails. See text for details.

Now using equations 5 and 2 we may calculate the excitation rates from the $v = 0 \cdots 4$ vibrational levels, and fit them with the form given in equation 3. This gives the coefficients shown in table 5.

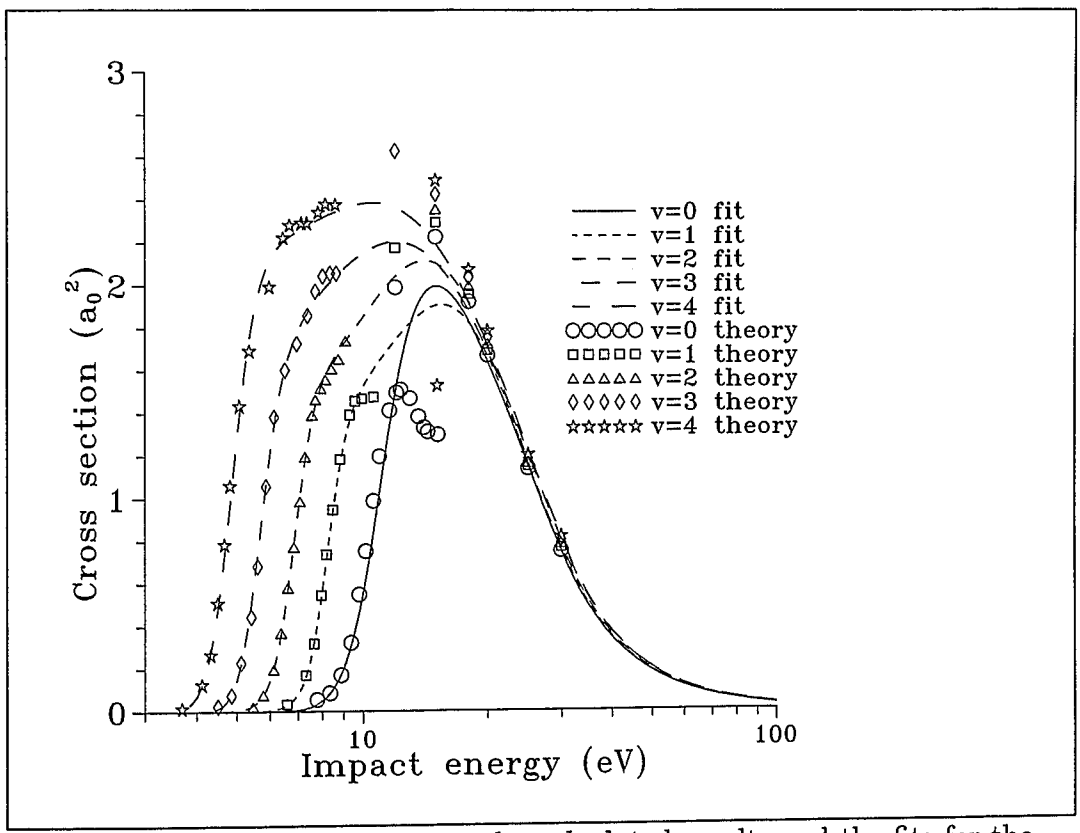

Figure 3: Comparison between the calculated results and the fits for the electron impact excitation of the $b^3\Sigma$ state. The symbols are calculated results (Stibbe-Tennyson at low energy, Rescignio-Schneider at high energy); the lines are the fits discussed in the text.

Vib. level no.	1	b^3 state
-0.2773725E+02	0.1142619E+02	-0.7106961E+01
0.2912997E+01	-0.8136092E+00	0.1439587E+00
-0.1527382E-01	0.8835154E-03	-0.2138525E-04
Vib. level no.	2	b^3 state
-0.2589590E+02	0.9308846E+01	-0.6111786E+01
0.2716542E+01	-0.8153286E+00	0.1517351E+00
-0.1666904E-01	0.9884728E-03	-0.2437205E-04
Vib. level no.	3	b^3 state
-0.2440907E+02	0.7305546E+01	-0.4716134E+01
0.2144935E+01	-0.6726041E+00	0.1298935E+00
-0.1467502E-01	0.8889656E-03	-0.2228626E-04
Vib. level no.	4	b^3 state
-0.2324716E+02	0.5829252E+01	-0.3744745E+01
0.1758024E+01	-0.5765017E+00	0.1150978E+00
-0.1331038E-01	0.8201187E-03	-0.2082853E-04
Vib. level no.	5	b^3 state
-0.2231170E+02	0.4660081E+01	-0.2898884E+01
0.1370694E+01	-0.4659871E+00	0.9578992E-01
-0.1131127E-01	0.7077043E-03	-0.1818595E-04

Table 5: The fitting parameters b_k (equation 3) for the excitation of the $b^3\Sigma$ state in the order

b_0 b_1 b_2

b_3 b_4 b_5

b_6 b_7 b_8

Unfortunately, this only gives rates for excitation from the first five vibrational levels of the ground state. We make an estimate of the rates for excitation from higher levels as follows. We consider each of the coefficients in table 5 as a function of the vibrational level number $n(= v+1)$, and fit each coefficient for $n = 2 \cdots 5$ as a quadratic in n. This enables us to extrapolate to higher n, or equivalently v. Explicitly, we have, for $n \geq 2$ ($v \geq 1$)

$$
\begin{aligned}
b_0 &= -29.6523 + 2.15635n - 0.137843n^2 \\
b_1 &= +14.4677 - 3.00199n + 0.208532n^2 \\
b_2 &= -9.59335 + 2.02314n - 0.137448n^2 \\
b_3 &= +4.05287 - 0.764931n + 0.046069n^2 \\
b_4 &= -1.12163 + 0.17078n - 0.00805247n^2 \\
b_5 &= +0.194018 - 0.0226971n + 0.00063343n^2 \\
b_6 &= -0.0200807 + 0.00173489n + 1.27242 \times 10^{-6} n^2 \\
b_7 &= +0.00113472 - 6.85277 \times 10^{-5} n - 3.2268 \times 10^{-6} n^2 \\
b_8 &= -2.68926 \times 10^{-5} + 1.02722 \times 10^{-6} n + 1.39197 \times 10^{-7} n^2
\end{aligned}
$$

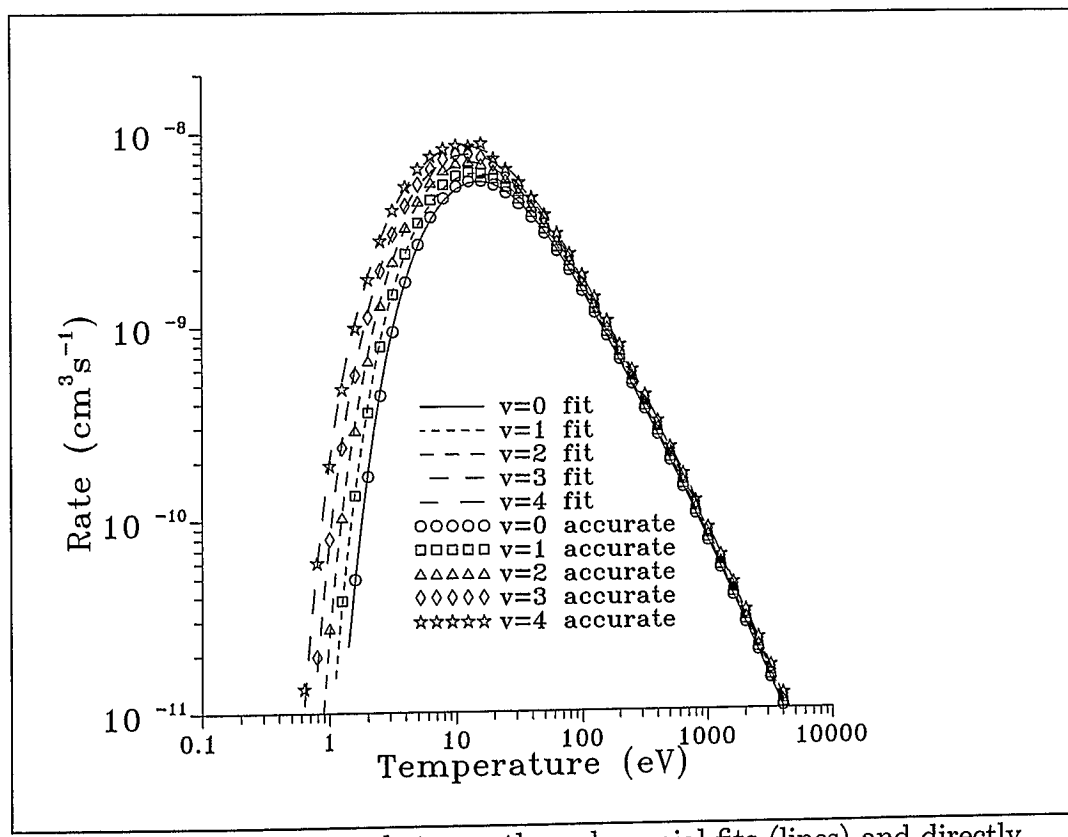

Figure 4: Comparison between the polynomial fits (lines) and directly calculated rates (symbols) for $v = 0 \cdots 4$.

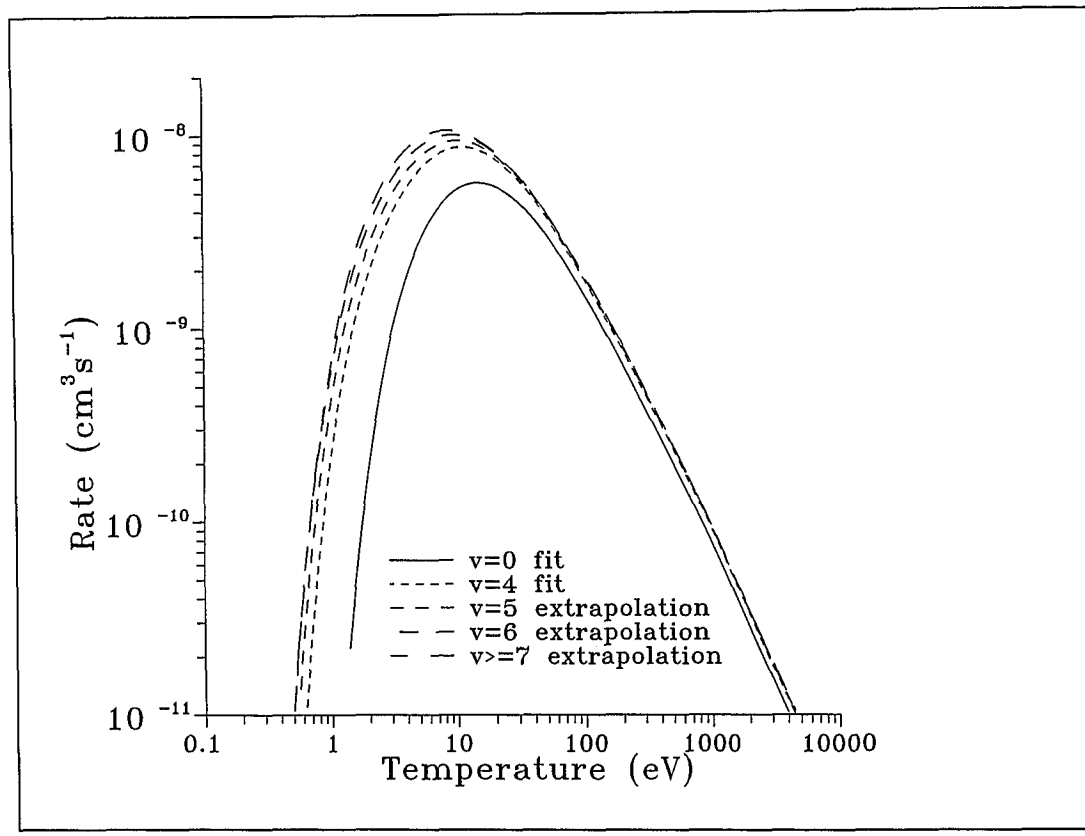

Figure 5: The rates for $v = 0, 4, 5, 6$ and $v \geq 7$.

This procedure has no physical justification, and we do not trust it beyond $n = 8$. For $n > 8$ we assume that the rates are all identical to the $n = 8$ ($v = 7$) rate. In due course a better extrapolation procedure will be developed. Some details of these rates are shown in figures 4 and 5.

10 Appendix 4 The streams

I give a list of the input and output streams used in the calculation, with a brief description of the content of the corresponding file. (The code allocates `stream` n to the file `fort.`n). I also indicate the section where more details are given.

stream 7 Input to define P space (Section 3)

stream 10 Input $i, j, M(i, j)$ for foreign matrix (Section 5)

stream 12 $j, i, \mathrm{M}(j, i)$ after removal of fixed densities, and permutation to isolate the P space (Section 3)

stream 17 N, N_P fullowed by N rows of the form i, `ipq`(i), `ipqf`(i), where i is the final index in M, `ipq`(i) the original index (after removal of

fixed densities, but before permutation to isolate the P space), and $\texttt{ipqf}(i)$ is the original index after permutation; i e the state at i in M corresponds to the species with original label $\texttt{ipqf}(i)$, as listed on stream 21. (Section 3)

stream 21 First, details of the state enumeration and permutation, as described above, followed by $l - K$ lines of the form i, x, y, a, b, e where:

i is a running index

x is the ith eigenvalues of the full matrix M

y is the ith eigenvalue of $\mathrm{M}_{\mathrm{eff}}$ if $i \leq N_P$

y is the $i - N_P$th eigenvalue of M_Q if $i > N_P$

a is the ith component of the nevx'th eigenvector of M (see input for definition of nevx).

b is the ith component of the nevx'th eigenvector of $\mathrm{M}_{\mathrm{eff}}$ for $i \leq N_P$. If $\texttt{nevx} > N_P$, this column is zero. $b = 0$ if $i > N_P$.

e is the error associated with the ith P state $(1 \leq i \leq N_P)$ or $i - N_P$th Q state $(N_P + 1 \leq i \leq N_P + N_Q)$. For the P states the error given is $\epsilon_{\mathrm{tot}}^{(i)}$; for the Q states $\epsilon_4^{(i-N_P)}$ is given. (Section 3)

stream 22 $j, i, \mathrm{M}_{\mathrm{eff}}(j,i)$ for use in the CR model (Section 3)

stream 23 $i, \Gamma_{\mathrm{P}}(i)$ for use in the CR model (Section 3)

stream 25 $i, \Gamma_{\mathrm{CR}}(i)$ in its permuted order (Section 3)

stream 32 $j, i, \mathrm{M}_Q(j,i)$ for use in the CR model (Section 3)

stream 33 $j, i, \left[\mathrm{M}_Q^{-1}\mathrm{V}\right](j,i)$ (Section 3)

stream 34 $j, i, \left[\delta\mathrm{T}_P^{-1}\right](j,i)$ (Section 3)

stream 35 $j, i, \left[\mathrm{HM}_Q^{-1}\right](j,i)$ (Section 3)

stream 36 $j, i, \left[\Delta\mathrm{T}_Q^{-1}\right](j,i)$ (Section 3)

stream 45 The energy rate matrix in the original order; (the analogue of stream 48). (Section 4)

stream 47 $i, \texttt{isn}(i)$, where i is the *original* species index, and $\texttt{isn}(i) = 0$ if state i is kept in the final matrix, $\texttt{isn}(i) = 1$ state i is removed. This information is written twice, omce from the rate calculation, once from the energy rate calculation. (Section 3)

stream 48 $j, i, \mathbf{M}(j,i)$, the full matrix, before removal of the fixed densities. (Section 3)

stream 49 $j, i, \mathbf{M}(j,i)$ after removal of fixed densities, in its original order. (Section 3)

stream 51 The energy rate matrix after the removal of the fixed densities; (the analogue of stream 49). (Section 4)

stream 60 $i, j, \mathbf{U}_{\text{eff}}(i,j)$, the effective $l \times l'$ energy rate matrix. See equation 58 *etc.* (Section 4)

stream 61 $j, \sum_i \mathbf{U}_{\text{eff}}(i,j), \bar{E}(j) = -\sum_i \mathbf{U}_{\text{eff}}(i,j)/\mathbf{M}_{\text{eff}}(j,j)$, the effective total electron energy loss rate/P space species (Section 4)

stream 70 $i, \texttt{colsum}(i), \texttt{sn}(i)$, where $\texttt{colsum}(i) = \sum_j K(j) M_{j,i}$, with $K(j)=$ number of nuclei in species j, and $\texttt{sn}(i) = \sqrt{\sum_j M_{j,i}^2}$. If $\texttt{colsum}(i)/\texttt{sn}(i) > 10^{-14}$ a diagnostic message is also written on `stdout`. This is only relevant if no heavy particle densities are fixed. (Section 3)

stream 77 $j, \bar{E}(j), \sum_i \mathbf{U}(i,j), -\mathbf{M}(j,j)$ with $\bar{E}(j) = -\sum_i \mathbf{U}(i,j)/\mathbf{M}(j,j)$, the effective total electron energy loss rate/species (Section 4)

stream 78 $j, i, \bar{E}(j,i), \mathbf{U}(j,i), \mathbf{M}(j,i)$ $\mathbf{U}$ (equation 54) is the analogue of $\mathbf{M}$, (equation 13). $\bar{E}(j,i) = \mathbf{U}(j,i)/\mathbf{M}(j,i)$ is the mean electron loss associated with the process $j \leftarrow i$. (Section 4)

stream 79 $i, \bar{E}_i, \Xi_E(i), \Gamma(i)$ in the permuted order. $\bar{E}_i = \Xi_E(i)/\Gamma(i)$ is the mean electron energy loss associated with the source i. (Section 4)

stream 80 $j, i, \mathbf{V}(j,i), \mathbf{H}(i,j)$ (Section 3)

stream 81 $j, i, \mathbf{M}_Q^{-1}(j,i)$ (Section 3)

stream 87 Accuracy data (Section 5)

stream 90 Gives similar details to stream 99, but in the form i, j, k, R, q, where the k'th rate with value R contributes to $\mathbf{M}_{ij}$ and corresponds to a process which gives q nuclei. (Section 3)

stream 91 i, e_i, f_i, where e_i is the real part, and f_i the imaginary part of the i'th eigenvalue of the *permuted* matrix $\mathbf{M}$. The eigenvalues are arranged in order of increasing absolute value, and the corresponding eigenvectors are written on stream 93. (Section 3)

stream 92 is identical to stream 91, except that the eigenvectors are those of the *unpermuted ie* the states are in their *original* order *cf* stream 49. The corresponding eigenvectors are on stream 94. (Section 3)

stream 93 $i, j, v_i^{(j)}, w_i^{(j)}$, where $v_i^{(j)}$ is the real part, and $w_i^{(j)}$ the imaginary part of the i'th componenent of the eigenvector of the *permuted* matrix $\mathbf{M}$, associated with the j'th eigenvalue of $\mathbf{M}$, where the eigenvalues are arranged in order of increasing absolute value. (Section 5)

stream 94 is identical to stream 93, except that the eigenvectors are those of the *unpermuted ie* the states are in their *original* order *cf* stream 49. (Section 5)

stream 95 This is the exact analogue of stream 97, but dispalys the singlet-triplet energy rates. It is not written if `stf`=0.

stream 96 The non-zero elements of the permutation matrix which operates on the original ordering of states to give the final ordering. (Section 3)

stream 97 Data on the singlet-triplet rates
$j, i, C_{st}(i,j), F_{st}(i,j), C_{ts}(j,i), F_{ts}(j,i), \Delta E, j_s, i_t$, where:

i is the triplet index, j is the singlet index

$C_{st}(i,j)$ is the excitation rate coefficient from the singlet state labelled by j to the triplet state labelled by i

$F_{st}(i,j)$ is the de-excitation rate coefficient from the singlet state labelled by j to the triplet state labelled by i

$C_{ts}(j,i)$ is the excitation rate coefficient from the triplet state labelled by i to the singlet state labelled by j

$F_{ts}(j,i)$ is the de-excitation rate coefficient from the triplet state labelled by i to the singlet state labelled by j

ΔE = (Binding energy of triplet state i_t − Binding energy of singlet state j_s)

j_s, i_t, indices for the singlet and triplet binding energies

stream 97 is not written if `stf`=0. (Section 3)

stream 98 The individual energy loss rates, the analogue of stream 99 in the form $\bar{E}_{k,j}$,<index>,$\mathcal{S}_j^k$, <description>, where $\bar{E}_{k,j} = \mathcal{S}_j^k / \mathcal{R}_j^k$ is the mean electron energy loss/process. (Section 4)

stream 99 All the non-zero individual rates used in the code are written out and identified both by a brief description and an index k. Those marked N/A are not used. (Section 3)

11 References

Allison AC, Dalgarno A, 1970; Atomic Data **1**, 289.

Bardsley JN, Wadehra JM (1979): Phys Rev **A20**, 1398

Celiberto R, Janev RK (1995): *'Analytical representation of electron impact excitation cross sections of vibrationally excited H_2 and D_2 molecules'* INDC(NDS)–333.

Greenland PT, 2000 'Collisional-Radiative models with molecules', to appear in *Proc Roy Soc.*

Greenland PT and Reiter D, 1996: 'The rôle of molecular hydrogen in plasma recombination', Jül-3258 ISSN 0944-2952 (Forschungszentrum Jülich).

Greenland PT and Reiter D, 1998: Contrib Plasma Phys, **38**, 302.

Janev RK, Langer WD, Evans Jr K, Post Jr DE (1987) 'Elementary processes in hydrogen-helium plasmas' Springer-Verlag (Berlin).

Johnson LC, 1972 The Astrophysical Journal **174** 227

Krasheninnikov SI, Pigarov A Yu and Sigmar DJ, 1996: Phys. Letters A **214**, 258.

Krasheninnikov SI, Pigarov A Yu, Soboleva TK and Sigmar DJ, 1997: J. Nucl. Mat. **241-243**, 283.

Reiter D, in "Atomic and Plasma-Material Interaction Processes in Controlled Thermonuclear Fusion", Ed. Janev RK, Drawin HD, Elsevier Science Publishers, 1993

Reiter D, May Chr, Baelmans M, Börner P, 1997: J. Nucl. Mat. **241-243**, 342

Rescignio TN and Schneider BI (1988): J Phys B (At Mol Phys) **21** L691.

Sawada K, Fujimoto T, 1995: J.Appl.Phys. **78**, 2913.

Stephens TL and Dalgarno A, 1972: J Quant Spectrosc Radit Trans **12**,569.

Stibbe DT and Tennyson J (1998): New J. Phys. **1**, 2.1-2.9.

Wünderlich D (2000): *Anwendung und Erweiterung eines Stoß-Strahlungs-Modells für H_2 und H.* Diplomarbeit des Lehrstuhles für Experimentalle Plasmaphysik, Universität Augsburg, Germany.

Forschungszentrum Jülich

Jül-3858
April 2001
ISSN 0944-2952